Studies on Litihum Ion Transfer at Positive-electrode/Electrolyte Interface(Dissertation_全文)

AUTHOR(S):

Yamada, Izumi

Studies on Lithium Ion Transfer at Positive-electrode/Electrolyte Interface

Izumi Yamada

2007

Studies on Lithium Ion Transfer at Positive-electrode/Electrolyte Interface

Izumi Yamada

Department of Energy and Hydrocarbon Chemistry
Graduate School of Engineering
Kyoto University

2007

PREFACE

This thesis is a compilation of studies on lithium ion transfer at positive-electrode / electrolyte interface that were carried out by the author under the supervision of Professor Zempachi Ogumi at Department of Energy and Hydrocarbon Chemistry, Graduates School of Engineering, Kyoto University during 2002 -2007.

The author wishes to express her sincere gratitude to Professor Zempachi Ogumi for his continuing guidance, valuable suggestions, and fruitful discussions throughout this work. The author wishes to thank Professor Takashi Kakiuchi and Professor Koichi Eguchi, Graduate School of Engineering, Kyoto University, for their helpful comments and discussions.

The author is deeply indebted to Dr. Takeshi Abe and Dr. Yasutoshi Iriyama for their continuing interest, hearty guidance, and fruitful discussions. The author is grateful to Professor Akimasa Tasaka (Doshisha University) and Dr. Minoru Inaba (Doshisha University) and all the members of Professor Ogumi's laboratory and Tasaka's laboratory.

The author wishes to express her specials thanks to her parents and brother for their continuous encouragement, support, and understanding toward accomplishing this thesis.

Finally, once again, the author wishes to express her heartfelt appreciation to Professor Zempachi Ogumi and Dr. Takeshi Abe for keeping watch over her fondly during the long hours that were invaluable for this work.

Izumi Yamada

CONTENTS

GENERAL INTRODUCTION

Background of the work

1. Rechargeable lithium-ion batteries

Rechargeable lithium-ion batteries have received considerable interest due to their high energy density. In lithium-ion batteries, the charge and discharge reactions are based on the insertion and extraction of lithium-ion at both the positive and negative electrodes, i.e., simple lithium-ion transfer from the positive (negative) and negative (positive) electrodes via a lithium-ion-conductive electrolyte [1]. Graphitic carbon and lithium-containing 3d-transition metal oxides are used as negative and positive electrodes, respectively [2]. The charge reaction can be described as follows;

Positive electrode: $LiCoO_2 \rightarrow xLi^+ + xe^- + Li_{1-x}CoO_2$

Negative electrode: $xLi^+ + xe^- + C \rightarrow Li_xC$

Battery reaction: $LiCoO_2 + C \rightarrow Li_{1-x}CoO_2 + Li_xC$

Commercialized lithium-ion batteries show high average potentials exceeding 3.6 V, resulting in higher energy densities in terms of both weight and volume compared to other rechargeable batteries [3]. Lithium-ion batteries have been expected to be useful as power sources in next-generation hybrid electric vehicles (HEV) However there are some serious problems regarding safety, life cycle, rate performance, etc. for their practical use in HEV [4].

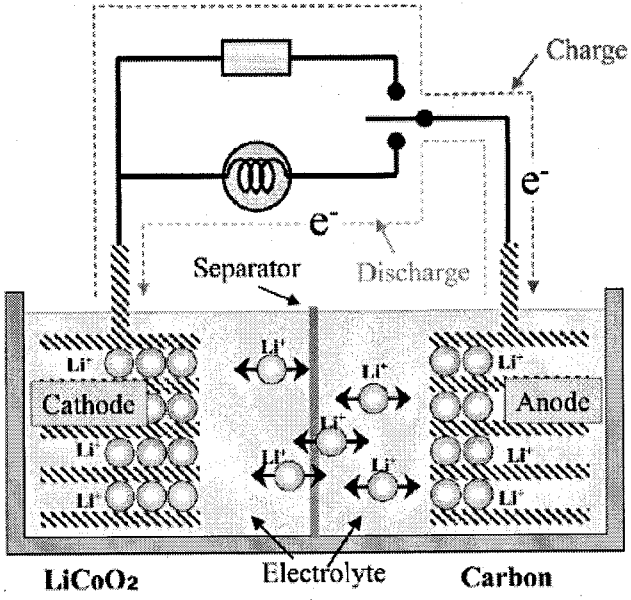

Fig.1 Principle of lithium-ion batteries.

The principle of lithium-ion batteries is very simple, as shown in Fig.1 [5]. As mentioned above, the charge and discharge reactions proceed by lithium-ion transfer between the negative and positive electrodes through electrolytes. Based on a consideration of the charge and discharge reactions, the internal resistance of lithium-ion batteries consists of 1) the electronic resistance between the current collector and electrode, 2) the electronic resistance of the electrodes, 3) lithium-ion diffusion through the active materials, 4) lithium-ion diffusion in the electrolyte, and 5) lithium-ion transfer at the electrode /electrolyte interface. The former electronic resistances are minimized by optimization in battery assembly, and therefore the rate performance of lithium-ion batteries depends on the rate of lithium-ion transfer. Lithium-ion diffusion in the active materials and electrolytes can be decreased, for example, by using fine particles and a thinner separator [6, 7]. Thus, the remaining process of lithium-ion transfer across the electrode / electrolyte interface should play an important role in the rate performance of lithium-ion batteries, although the mechanism of interfacial lithium-ion transfer reaction is not yet well understood. In addition to rate performance, the interfacial reaction at the electrodes, and particularly the positive electrode, is quite important for elucidating the mechanism of degradation in lithium-ion batteries [8-10]. Therefore, lithium-ion transfer at the positive electrode / electrolyte interface should be studied in detail.

2. Interfacial reaction at the positive electrode / electrolyte interface in lithium-ion batteries

Interfacial reactions at insertion electrodes are quite different compared to electron transfer reactions at metal electrodes. The interfacial reaction at insertion electrodes consists of multiple steps, such as the transport of solvated ions across an electric double layer, adsorption on the electrode surface, ion transfer, de-solvation, and ion insertion into the active material. This kind of process can also be found in amalgamation.

Amalgamation occurs through multi-step reactions and has been well studied [11-16]. Based on the literature, the rate-determining step of amalgamation in some systems is ion transfer, and therefore, de-solvation plays an important role [11-16].

2.1. Interfacial reaction at insertion electrodes

The interfacial reaction at insertion electrodes has been studied by some groups. Rainstrick et al. [17] studied lithium-ion transfer at a $Li_xNa_yWO_3$ / electrolyte interface and obtained the Nyquist plots given in Fig. 2. Only one semi-circle that was ascribed to charge transfer at the interface was observed. The temperature-dependence of the charge transfer resistances gave an apparent activation energy of ca. 50 $kJmol^{-1}$, regardless of the electrode potentials.

Bruce and Saidi [18, 19] proposed an "adion model" for the interfacial reaction, as represented in Fig. 3. In this model, interfacial reaction proceeds as follows:1) a solvated lithium-ion is partly de-solvated and adsorbed on the electrode surface, 2) a partly de-solvated lithium-ion diffuses toward intercalation sites across the interface, and 3) a lithium-ion is de-solvated completely and inserted into the host lattice. They proposed that the rate-determining step is lithium-ion insertion into the host lattice, and that the charge transfer reaction rate is partly controlled by the de-solvation step. On the basis of this adion model, Atanasov et al. [20] calculated the energies of lithium-ion transfer across the interface, and showed the existence of an activation barrier of de-solvation when lithium-ion is inserted from the electrolyte to the electrode. Bueno and Saidi [21] studied

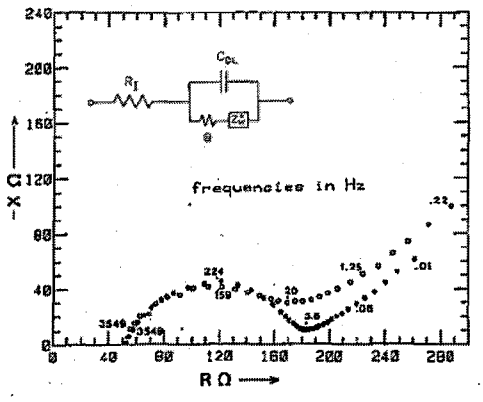

Fig. 2. Nyquist plots for $Li_yNa_xWO_3$ / 1M $LiAsF_6$-PC.

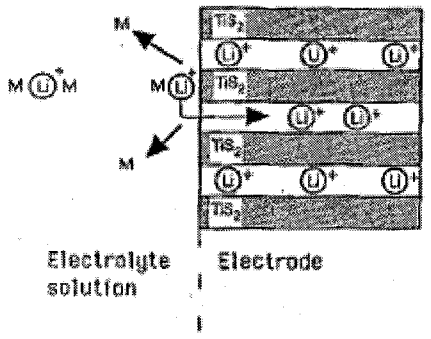

Fig. 3. Schematic representation of the adion mechanism of intercalation.

nano-structured insertion electrodes and proposed a model similar to the "adion" model.

In addition to the "adion model", interfacial ion transfer reactions have been studied by considering surface film formation [22], electron transfer [23], and various rate-determining steps [24]. However, composite porous electrodes that include binder and conductive additives have been used in the above studies, and therefore, it is very difficult to conduct systematic studies on interfacial ion transfer processes at electrodes, which has led to various interpretations for the lithium-ion transfer process at electrodes. By using binder-free electrodes such as highly oriented pyrolytic graphite (HOPG) and thin-film electrode prepared by plasma CVD, the rate-determining step for interfacial ion transfer at electrodes has been reported to be a de-solvation process [25, 26]. However, these studies have only considered negative electrodes.

It is also expected that de-solvation will play an important role in interfacial lithium-ion transfer at positive electrode.

2.2. Solvation

As mentioned above, de-solvation processes are very important for lithium-ion transfer process at electrodes in lithium-ion batteries. Therefore, the solvation of lithium-ion in organic electrolytes should be understood in detail. Organic electrolytes have been studied extensively. Gritzner [27-29] showed that ion-solvent interactions

should be treated as expanded Lewis-type donor-acceptor interactions.

Izutsu et al. [30] studied the solvation states of lithium-ion in the co-solvents of propylene carbonate (PC) and 1,2-dimethoxyethane (DME). They showed that the activities of lithium-ion in these electrolytes can be explained by the solvation abilities and dielectric constants of the solvents.

Based on the above studies, the state of solvated lithium ion is mainly affected by the donor number (electron-donating ability or solvation ability).

2.3. Orientation of positive materials

In addition to de-solvation processes, interfacial lithium-ion transfer should be influenced by other factors, including the anisotropic structures of the active materials. Some positive materials possess layered anisotropic structures.

Bates and co-workers [31, 32] fabricated $LiCoO_2$ thin films with different orientations by dc magnetron sputtering, and charge-discharge reactions of the resultant film electrodes were studied. However, there was no clear difference in charge-discharge performance. This is probably due to the many cracks or small grain sizes of the *c*-axis-oriented film electrode, which resulted in many lithium-ion insertion sites.

In contrast, Iriyama et al. [33] fabricated a well-crystallized $LiCoO_2$ thin film electrode with different orientations by pulsed laser deposition and showed that the orientation of $LiCoO_2$ affected the charge transfer resistance.

Garofalini and Garcia [34, 35] calculated lithium-ion transfer at a V_2O_5 / electrolyte interface and compared the ease of lithium-ion insertion/extraction and diffusivity between (001) plane and the amorphous phase. As a result, they showed that lithium-ions are inserted and diffuse more easily at the amorphous phase than at the (001) plane

Thus, interfacial lithium-ion transfer is greatly influenced by the orientation of positive electrodes. However, the details are not well understood.

3. Oxidation of electrolytes at positive electrodes

At higher potentials exceeding 4 V (vs. Li/Li^+), electrolytes are exposed to a strongly oxidative atmosphere. In addition, transition metal oxides of positive active materials in the state of full-charge should also be strongly oxidizing. Therefore, the reactivity between the positive electrode and the electrolyte should increase during charging.

The reactivity between organic solvents in the electrolyte and electrode is very important for the degradation of lithium-ion batteries. Therefore, tolerance toward electrolyte oxidation has been extensively studied mainly by linear sweep voltammetry (LSV) with an inert metal electrode such as Pt [36-38].

Aurbach and co-workers [39] studied the decomposition reaction of various electrolytes on Al, Pt, and Au electrodes with FTIR, EQCM, NMR, MS, and GCMS, and showed that electrolytes decomposed over 4 V (vs. Li/Li^+) regardless of the electrode used and that solvents, rather than anions, decomposed.

Joho and Novak [40] used SNIFTIR (Substractively Normalized Interfacial FTIR) to study electrolyte decomposition. In a comparison of PC and ethylene carbonate (EC), the oxidative reaction rate of EC was less than that of PC due to viscosity. They also showed that a solvent with a higher dielectric constant was selectively oxidized in mixed solvents.

Although the oxidative decomposition of electrolytes on model electrodes such as Pt is reported to give polymer-like decomposition products, many more studies using practical positive electrodes are necessary because the decomposition reaction may differ between model electrodes and transition metal oxides.

Jow and co-workers[41] showed that the oxidation potentials of electrolyte on $LiMn_2O_4$ and Pt and glassy carbon electrodes were different. Imhof and Novak [42] used DEMS (Differential Electrochemical MS) to study the oxidative decomposition of electrolyte by detecting CO_2 as a decomposition product. In this study, the oxidation potential of electrolyte was 4.2 V on $LiNiO_2$, but 4.8 V on $LiCoO_2$ and $LiMn_2O_4$.

Kanamura and co-workers [43-45] fabricated a thin-film electrode with no additives and studied the oxidative decomposition of electrolyte. The following results were obtained; 1) PC adsorbed on $LiCoO_2$ is oxidized to give organic compounds with

carboxylic group, 2) a portion of the carboxylic compounds exist on the electrode surface, and 3) the oxidation of PC starts at ca. 4.1 V (vs. Li/Li^+). In addition, they showed that the rate of oxidative decomposition changed although the decomposition products did not change according to the kind of anion.

Outline of the work

As noted above, reactions at the interface between a positive electrode and the electrolyte are very complicated. Although interfacial lithium-ion transfer is an essential reaction in a lithium-ion battery system, it is not yet well understood and many issues are not clear. To improve the battery performance for larger-scale power sources, higher rate performance is required. As mentioned above, rate performance depends on the reaction rates of charge and discharge, i.e., the speed of lithium-ion transfer. Therefore, a detailed understanding of the interfacial lithium-ion transfer reaction could lead to more advanced lithium-ion batteries with higher power and rate performance. The purpose of the present work was to clarify the kinetics of the lithium-ion transfer reaction at a structurally ordered interface using positive thin-film electrodes prepared by pulsed laser deposition. In particular, the present work focused on the effects of positive active materials and the kinds of electrolytes on interfacial reactions.

In Part 1, to elucidate the effects of positive materials on the interfacial lithium-ion transfer reaction, lithium-ion transfer at the $LiMn_2O_4$ and $LiCoO_2$ thin-film electrode / electrolyte interface was studied by AC impedance spectroscopy. The effects of the crystal structures and orientations of the positive materials are discussed in terms of the resistances and activation energies for interfacial lithium-ion transfer.

In Chapter 1, lithium-ion transfer at the interface between $LiMn_2O_4$ thin-film electrode and electrolyte was studied by AC impedance spectroscopy. $LiMn_2O_4$ thin film was fabricated by pulsed laser deposition (PLD). Nyquist plots gave no semi-circle at electrode potentials below 3.7 V(vs. Li/Li^+). At electrode potentials above 3.8 V, one

semi-circle appeared in the higher frequency region followed by diffusional behavior in the lower frequency region. This semi-circle was assigned to the charge transfer resistance due to interfacial lithium-ion transfer. The charge transfer resistance decreased with increasing electrode potentials up to 4.0 V and then increased. The temperature-dependence of the resistance gave an activation energy of about 50 $kJmol^{-1}$, indicating that a high activation barrier exists at the $LiMn_2O_4$ electrode / electrolyte interface for lithium-ion transfer.

In Chapter 2, the effect of the crystal structures of the positive materials on lithium-ion transfer at the interface between a positive electrode and electrolyte was studied by AC impedance spectroscopy. Thin-film electrodes of $LiCoO_2$, a layered 2-dimensional structure, and $LiMn_2O_4$, a spinel-typed 3-dimensional structure, were fabricated by PLD. The charge transfer resistances on $LiMn_2O_4$ were smaller than those on $LiCoO_2$, indicating that the number of sites at the interface influenced charge transfer resistances. With cycling, the charge transfer resistances on $LiMn_2O_4$ were almost unchanged while those on $LiCoO_2$ gradually increased which suggested the formation of a surface film. Activation energies evaluated from the temperature-dependence of charge transfer resistances were similar and a large activation barrier is assumed to exist at the interface, regardless of the positive materials used. These results suggest that charge transfer resistance is influenced by the crystal structures of positive materials. In addition, the crystal structure of positive materials has no influence on the activation energy for interfacial lithium-ion transfer.

In Chapter 3, the effect of the orientation of $LiCoO_2$ on lithium-ion transfer at the interface between electrode and electrolyte was studied by AC impedance spectroscopy. *C*-axis-oriented and randomly oriented $LiCoO_2$ thin films were fabricated by changing the deposition time of PLD. The charge transfer resistance on *c*-axis-oriented thin film was 10-fold greater than that on randomly oriented thin film. In contrast, the activation energies evaluated from the dependence of the charge transfer resistance were similar regardless of the orientation. Controlling the orientation of $LiCoO_2$ is very important improving battery performance.

In Part 2, to elucidate the effects of the electrolytes on the interfacial lithium-ion transfer reaction, lithium-ion transfer at the interface between the positive electrode and

various electrolytes was studied by AC impedance spectroscopy. The effects of solvents and lithium salts are discussed in terms of resistances and activation energies for lithium-ion transfer.

In Chapter 4, the effect of the form of the electrolyte on lithium ion transfer at the interface between a $LiCoO_2$ electrode and a gel electrolyte was studied by AC impedance spectroscopy. The gel electrolyte was prepared by using polyvinylidene fluoride (PVdF) as a host matrix and polyethyleneglycol dimethyl ether (PEGDME) as a plasticizer, $LiCoO_2$ composite and thin-film electrodes were used as positive electrodes. For both the composite and thin-film electrodes, the impedance ascribed to lithium-ion transfer through the interface, i.e., charge transfer resistance, was observed in the mid to lower frequency regions in Nyquist plots. The charge transfer resistance decreased in the initial stage of charging up to about 3.9 V vs. Li/Li^+ and then increased from about 4 V. The charge transfer resistances for $LiCoO_2$ thin-film electrodes were much greater than those for $LiCoO_2$ composite electrodes due to their small reaction area. The activation energies for lithium-ion transfer increased with an increase in the molecular weight of PEGDME. Therefore, the plasticizer also plays an important role in lithium-ion kinetics at the electrode. A higher molecular weight for the plasticizer should give safrer lithium-ion batteries, but the lithium-ion kinetics will become slower.

In Chapter 5, the effect of the electrolyte on lithium-ion transfer at the interface between a positive electrode and liquid electrolyte was studied by AC impedance spectroscopy. The dependence of charge transfer resistance on electrode potentials varied with the solvent, while no changes were observed with changes in the lithium salts. The onset electrode potentials when charge transfer resistances increased depended on the kind of solvent, indicating that tolerance toward oxidative decomposition is influenced by the solvent. The activation energies for lithium-ion transfer as evaluated from the temperature-dependence of charge transfer resistances varied according to the solvation abilities of the solvents toward lithium-ion. These results indicate that interfacial lithium-ion transfer tends to be influenced more by solvents than by anions.

References

[1] M. Winter, J.O. Besenhard, M.E. Spahr and P. Novak, *Adv.Mater.*, **10**(1998), 725

[2] K. Brandt, *Solid State Ionics,* **69**(1994), 173

[3] J.M. Tarascon and M. Armand, *Nature,* **414**(2001), 359

[4] K. Smith and C.-Y. Wang, *J. Power Sources,* **160**(2006), 662

[5] Y. Nishi, *Chem. Rec.,* **1**(2001), 406

[6] J.B. Bates, N.J. Dudney, B. Neudecker, A. Ueda and C.D. Evans, *Solid State Ionics,* **135**(2000), 33

[7] B.J. Neudecker, N.J. Dudney and J.B. Bates, *J. Electrochem. Soc.,* **147**(2000), 517

[8] J. Vetter, P. Novak, M.R. Wagner, C. Veit, K.-C. Moller, J.O. Besenhard, M. Winter, M. Wohlfhart-Mehrens, C. Vogler and A. Hammouche, *J. Power Sources,* **147**(2005), 269

[9] B. Markovsky, A. Rodkin, Y.S. Cohen, O. Palchik, E. Levi, D. Aurbach, H.-J. Kim and M. Schmidt, *J. Power Sources,* **119-121**(2003), 504

[10] C.H. Chen, J. Liu and K. Amine, *Electrochem. Comm.,* **3**(2001), 44

[11] R.M. Hurd, *J. Electrochem. Soc.,* **109**(1962), 327

[12] M. Sluyters-Rehbach and J.H. Sluyters, *Electrochim. Acta.,* **33**(1988), 983

[13] A.S. Baranski and W.R. Fawcett, *J. Chem. Soc. Faraday Trans. 1,* **76**(1980), 1962

[14] A.S. Branski and W.R. Fawcett, *J. Chem. Soc. Faraday Trans. 1,* **78**(1982), 1279

[15] W.R. Fawcett, *Langmuir,* **5**(1989), 661

[16] J. Broda and Z. Galus, *J. Electroanal. Chem.,* **198**(1986), 223

[17] I.D. Raistrick, *Solid State Ionics,* **9-10**(1983), 425

[18] P.G. Bruce and M.Y. Saidi, *J. Electroanal. Chem.,* **322**(1992), 93

[19] P.G. Bruce and M.Y. Saidi, *Solid State Ionics,* **51**(1992), 187

[20] M. Atanasov, C. Daul, J.L. Barras, L. Benco and E. Deiss, *Solid State Ionics,* **121**(1999), 165

[21] P.R. Bueno and E.R. Leite, *J. Phys. Chem. B,* **107**(2003), 8868

[22] M. Thomas, P.G. Bruce and J.B. Goodenough, *J. Electrochem. Soc.,* **132**(1985), 1521

[23] F. Nobli, R. Tossici, R. Marassi, F. Croce and B. Scrosati, *J. Phys. Chem. B,* **106**(2002), 3909

[24] M. Nakayama, H. Ikuta, Y. Uchimoto and M. Wakihara, *J. Phys. Chem. B,* **107**(2003), 10603

[25] T. Abe, H. Fukuda, Y. Iriyama and Z. Ogumi, *J. Electrochem. Soc.*, **151** (2004) A1120

[26] Z. Ogumi, T. Abe, T. Fukutsuka, S. Yamate and Y. Iriyama, *J. Power Sources*, **127** (2004) 72

[27] G. Gritzner, *Inorg. Chim. Acta.,* **24**(1977), 5

[28] G. Gritzner, *J. Mol. Liq.,* **73-74**(1997), 487

[29] G. Gritzner, *Electrochim. Acta.,* **44**(1998), 73

[30] K. Izutsu, T. Nakamura, K. Miyoshi and K. Kurita, *Electrochim. Acta.,* **41**(1996), 2523

[31] F.X. Hart and J.B. Bates, *J. Appl. Phys.,* **83**(1998), 7560

[32] J.B. Bates, N.J. Dudney, B.J. Neudecker, F.X. Hart, H.P. Jun and S.A. Hackney, *J. Electrochem. Soc.,* **147**(2000), 59

[33] Y. Iriyama, M. Inaba, T. Abe and Z. Ogumi, *J. Power Sources*, 94 (2001) 175

[34] M.E. Garcia and S.H. Garofalini, *J. Electrochem. Soc.,* **146**(1999), 840

[35] S.H. Garofalini, *J. Power Sources,* **110**(2002), 412

[36] K. Nishimura, M. Mizumoto, H. Momose and T. Horiba, *DENKI KAGAKU,* **63**(1995), 802

[37] M. Ue, A. Murakami and S. Nakamura, *J. Electrochem. Soc.,* **149**(2002), A1572

[38] B. Rasch, E. Cattaneo, P. Novak and W. Vielstich, *Electrochim. Acta,* **36**(1991), 1397

[39] M. Moshkovich, M. Cojocaru, H.E. Gottlieb and D. Aurbach, *J. Electroanal. Chem.,* **497**(2001), 84

[40] F. Joho and P. Novak, *Electrochim. Acta.,* **45**(2000), 3589

[41] S.S. Zhang, K. Xu and T.R. Jow, *Electrochem. Solid State Lett.,* **5**(2002), A92

[42] R. Imhof and P. Novak, *J. Electrochem. Soc.,* **146**(1999), 1702

[43] K. Kanamura, S. Toriyama, S. Shiraishi, M. Ohashi and Z. Takehara, *J. Electroanal. Chem.,* **419**(1996), 77

[44] K. Kanamura, *J. Power Sources,* **81-82**(1999), 123

[45] K. Kanamura, T. Umegaki, M. Ohashi, S. Toriyama, S. Shiraishi and Z. Takehara, *Electrochim. Acta,* **47**(2001), 433

PART I

Effects of Positive Electrode Materials on Interfacial Lithium Ion Transfer

CHAPTER 1

Lithium-Ion Transfer at $LiMn_2O_4$ Thin Film Electrode Prepared by Pulsed Laser Ablation

1.1. Introduction

Lithium-ion batteries have been used in portable electronic devices due to their high energy densities. Not only further improvement of Li-ion batteries in electronic devices but also hybrid electric vehicles (HEV) employing Li-ion batteries are the major driving force behind recent R&D of Li-ion batteries.

Fast charge and discharge reactions are required for a practical use of Li-ion batteries in HEV, and therefore, kinetic studies of Li-ion transfer at positive and negative electrodes are essential in addition to Li-ion transport properties in active materials or Li-ion conductive electrolytes. Latter issues have been well investigated mainly by reporting Li-ion diffusion coefficients in active materials [1] and electrolytes [2, 3]. Although transport properties of Li-ion batteries play an important role for fast charge and discharge reactions, the diffusion paths of electrodes and electrolytes can be shortened by practical ways. Employment of thin composite electrodes and separator will enhance the reaction rate of Li-ion batteries due to decrease of internal resistances caused by low Li-ion

conductivities of electrolyte. In commercialized Li-ion batteries, composite electrodes are rolled or stacked to enhance reaction sites for Li-ion insertion and extraction, leading to the lower charge (Li-ion) transfer resistances. However, thinner composite electrodes decrease the reaction sites resulting in larger charge transfer resistances and thus former issues should be focused.

Structurally ordered interface is essential for elucidation of Li-ion transfer at electrode/electrolyte interface. Flat and homogeneous thin film electrodes are ideal for fabrication of the ordered interface. We have prepared $LiCoO_2$ thin films [4-6], $LiMn_2O_4$ [7], MoO_3 [8] by pulsed laser deposition (PLD), and lower to highly crystallized carbonaceous thin films [9-13] by plasma assisted chemical vapor deposition. Intrinsic electrochemical properties have been well clarified by use of these film electrodes.

$LiMn_2O_4$ possesses a spinel-type structure and gives three-dimensional Li-ion paths, and therefore, reaction sites can be well defined by use of $LiMn_2O_4$ thin film electrode. Hence, $LiMn_2O_4$ thin film is very suitable for studies on Li-ion transfer at electrode/electrode. In this communication, we report Li-ion transfer at $LiMn_2O_4$ thin film electrode by AC impedance spectroscopy and show high activation barrier at the electrode/electrolyte interface for the first time.

1.2. Experimental

$LiMn_2O_4$ thin films were prepared by pulsed laser deposition using KrF excimer laser of a wavelength of 248 nm (Japan Storage Battery, EXL-210). Substrate was a polished Pt plate whose temperature was kept at 973 K. Detailed preparation conditions were reported elsewhere [7]. X-ray diffraction (XRD) measurement was conducted by Rint-2500 (Rigaku) equipped with a graphite monochrometer with a scintillation detector. Typical working conditions were 40 kV and 250 mA with a scanning speed of 0.125 s.

Electrochemical properties of the $LiMn_2O_4$ thin film electrode were studied by cyclic voltammetry employing a three-electrode cell (lithium metal was used as counter and reference electrodes) by HSV-100 (HOKUTO-DENKO Inc). Unless otherwise stated,

potentials are referred to lithium metal. Electrolytes used were propylene carbonate (PC) or a mixture of ethylene carbonate (EC) and diethyl carbonate (DEC) (vol. 1:1) containing 1 mol dm^{-3} $LiClO_4$.Lithium-ion transfer at $LiMn_2O_4$ thin film electrode was studied by AC impedance spectroscopy using (Radiometer, VoltaLab40) over the frequency region from 100 kHz to 10 mHz employing the same three-electrode cell.

All experiments were conducted under Ar atmosphere.

1.3. Results and discussion

Figure 1 shows XRD patterns of a film deposited on Pt at 973 K for 3 h. Number on peaks denote to index *hkl*. XRD pattern is identical to the literature [14]. Very sharp peaks appear as is given in Fig. 1, indicating that the resultant $LiMn_2O_4$ thin film is well crystallized. Redox behavior of the thin film electrode was examined by cyclic voltammetry in 1 mol dm^{-3} $LiClO_4$ / PC. As is shown in Fig. 2, the thin film shows redox behaviors with two couples of redox peaks at around 4.0 and 4.1 V. Since electroactive species are deposited on the electrode surface, the species should show the redox behavior of adsorbate, i.e., oxidation and reduction peaks are symmetrical. However, the voltammogram shows somewhat diffusional behavior. The peak separation was not zero but about 30 mV. This is because the amount of active species ($LiMn_2O_4$) deposited on Pt disk (current collector) is too much and the diffusional behavior of Li-ion through $LiMn_2O_4$ thin film was observed. This small peak separation means that the ohmic drop is small and therefore the electric conductivity of the $LiMn_2O_4$ thin film electrode is high enough for electrochemical measurements.

In Fig. 3 are shown Nyquist plots at given potentials ranging 3.6 - 4.2 V. At potential of 3.6 V, no semi-circle but only blocking electrode behavior appeared. No oxidation and reduction currents were observed in cyclic voltammogram given in Fig. 2, and therefore, blocking electrode behavior at 3.6 V is quite valid. One semi-circle appeared in the higher frequency regions followed by a diffusional behavior in the lower frequency regions at potentials above 3.80 V. Although electric conductivity of $LiMn_2O_4$ is reported to be small

[15], a thickness of obtained $LiMn_2O_4$ thin film electrode is evaluated to be around 300 nm [7], and therefore electric resistance should be very small. Further, ohmic drop was found to be very small by cyclic voltammograms as mentioned above, and hence the semi-circles given in Fig. 3 are not ascribed to electric resistances of electrode. Semi-circles are dependent on electrode potentials and also salt concentration of electrolyte used, indicating that the semi-circles are derived from the relaxation process related with Li-ion. It is now clear from these facts and consideration that resistances of semi-circles in Fig. 3 are ascribed to charge (Li-ion) transfer resistances.

Figure 4 shows Li-ion transfer resistances against electrode potentials in 1 mol dm^{-3} $LiClO_4$ /PC (open circles) and EC+DEC (solid squares). Irrespective with electrolytes, the behaviors of Li-ion transfer resistances are almost the same; Li-ion transfer resistances decrease with increasing electrode potentials up to 4.0 V and then increased with increasing electrode potentials. Decrease of Li-ion transfer resistances is due to the increase of carrier concentration of Li-ion. At higher potentials corresponding to $Li_xMn_2O_4$ ($x < 0.5$), carrier concentration of Li-ion will decrease resulting in increase of Li-ion transfer resistances. At higher potentials, electrolyte decomposition may take place to form passivation film on $LiMn_2O_4$ thin film electrode. The passivation film also decreases reaction sites for Li-ion transfer at the $LiMn_2O_4$ electrode. To clarify the above two explanations, Li-ion transfer resistances were evaluated by decreasing electrode potentials from 4.2 to 3.6 V. The behavior of Li-ion transfer resistances against electrode potentials was quite reversible. When the passivation film is principally due to the increase of Li-ion transfer resistances, irreversible behaviors should be observed. Hence, carrier concentration is responsible for correlation between Li-ion transfer resistances and electrode potentials.

It should be noted that minimum values of Li-ion transfer resistance are around 80 - 100 cm^2 as given in Fig. 4. Atomic force microscopic study showed that the obtained $LiMn_2O_4$ thin film electrode was very flat and homogeneous, leading to the precise Li-ion transfer resistances. In contrast, by use of composite electrodes, reaction sites for Li-ion transfer at electrodes cannot be defined, and therefore one cannot obtain the exact values of Li-ion transfer resistances. The values of 80 - 100 cm^2 are very large for fast charge and

discharge reactions of Li-ion batteries. Hence, enhancement of reaction sites is essential for enhancement of rate performance of Li-ion batteries.

In Fig. 5, temperature dependency of Li-ion transfer resistances is given. By the least-square method, activation energy for Li-ion transfer resistances at a potential of 3.94 V was determined to be 50 kJ mol^{-1}. This value is very large as compared with those for Li-ion conduction in active materials and liquid electrolytes, indicating that high activation barrier should exist at interface between $LiMn_2O_4$ electrode / electrolyte.

1.4. Conclusions

Fabrication of structurally ordered interface consisting of $LiMn_2O_4$ thin film electrode and electrolyte gives precise studies on Li-ion transfer at $LiMn_2O_4$ electrode. Lithium-ion transfer resistances are clarified to be very large and large activation barrier at $LiMn_2O_4$ electrode/electrolyte interface becomes explicit. Enhancement of rate performance of Li-ion batteries can be attained by reducing the activation barriers at electrode/electrolyte interface, which will be reported elsewhere.

References

[1] For example, Van der Ven A. and G. Ceder, *Electrochem. Solid State Lett.*, 3, 301 (2000).

[2] A. M. Stephan and Y. Saito, *Solid State Ionics*, 148, 475 (2002).

[3] H. Kataoka, Y. Saito, T. Sakai, S. Deki, and T. Ikeda, *J. Phys. Chem. B* 105, 2346 (2001).

[4] Y. Iriyama, M. Inaba, T. Abe, and Z. Ogumi, *J. Power Sources*, 94, 175 (2001).

[5] I. Yamada, T. Abe, Y. Iriyama, and Z. Ogumi, submitted.

[6] Z. Ogumi, T. Abe, and Y. Iriyama, *Solid State Ionics*: Trends in the new millenium, 3 (2002).

[7] M. Inaba, T. Doi, Y. Iriyama, T. Abe, and Z. Ogumi, *J. Power Sources*, 82, 554 (1999).

[8] Y. Iriyama, T. Abe, M. Inaba, and Z. Ogumi, *Solid State Ionics*, 135, 95 (2000).

[9] T. Abe, K, Takeda, T. Fukutsuka, Y. Iriyama, M. Inaba, and Z. Ogumi, *Electrochem. Commun.*, 4, 310 (2002).

[10] T. Abe, T. Fukutsuka, M. Inaba, and Z. Ogumi, *Carbon*, 1999, 37, 1165.

[11] T. Fukutsuka, T. Abe, M. Inaba, and Z. Ogumi, *Mol. Cryst. Liq. Cryst.*, 2000, 340, 517.

[12] T. Fukutsuka, T. Abe, M. Inaba, and Z. Ogumi, *J. Electrochem. Soc.* 2001, 148, A989.

[13] Z. Ogumi, T. Abe, S. Yamate, T. Fukutsuka, and Y. Iriyama, submitted.

[14] JCPDS No. 35-0782

[15] M. Nishizawa, T. Ise, H. Koshika, T. Itoh, and I. Uchida, *Chem. Mater.*, 12, 1367 (2000)

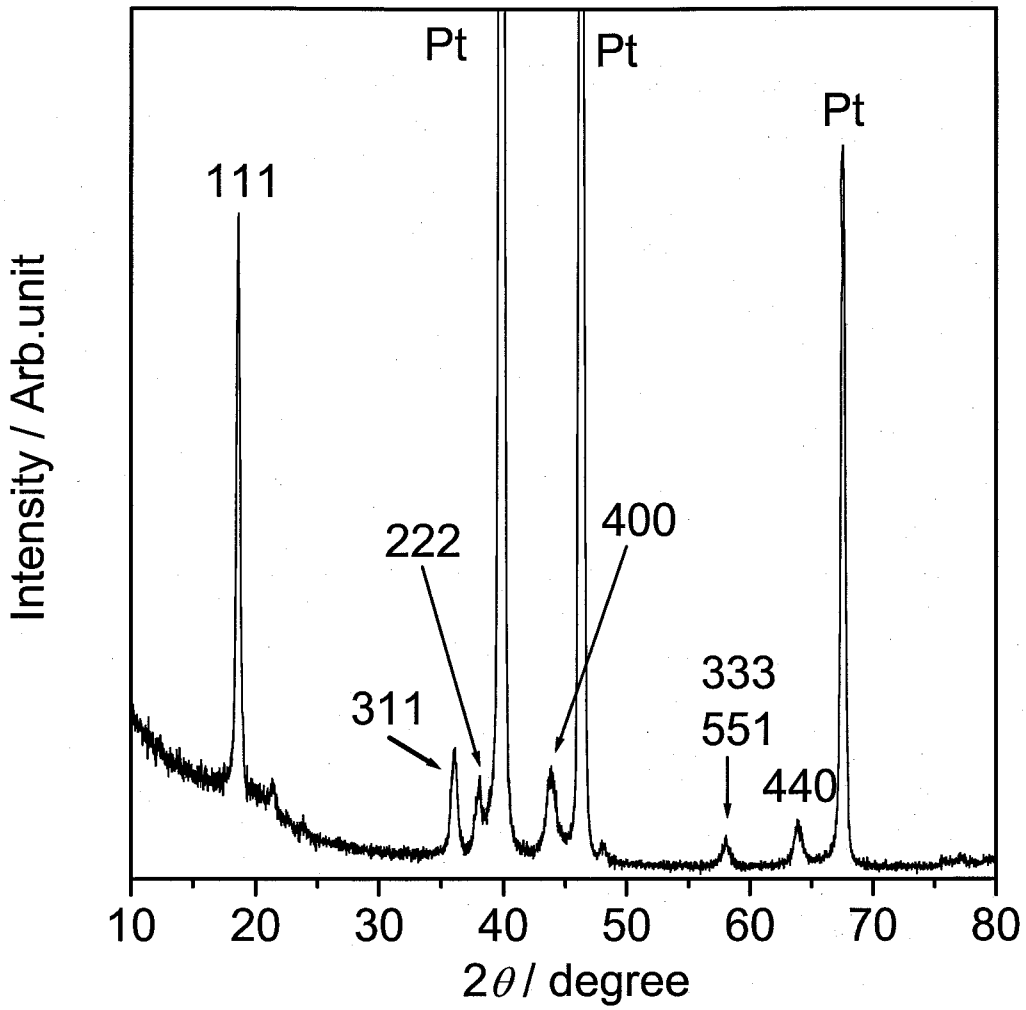

Fig. 1.1 X-ray diffraction pattern of $LiMn_2O_4$ thin film on Pt disk. Number on peaks denotes index *hkl*.

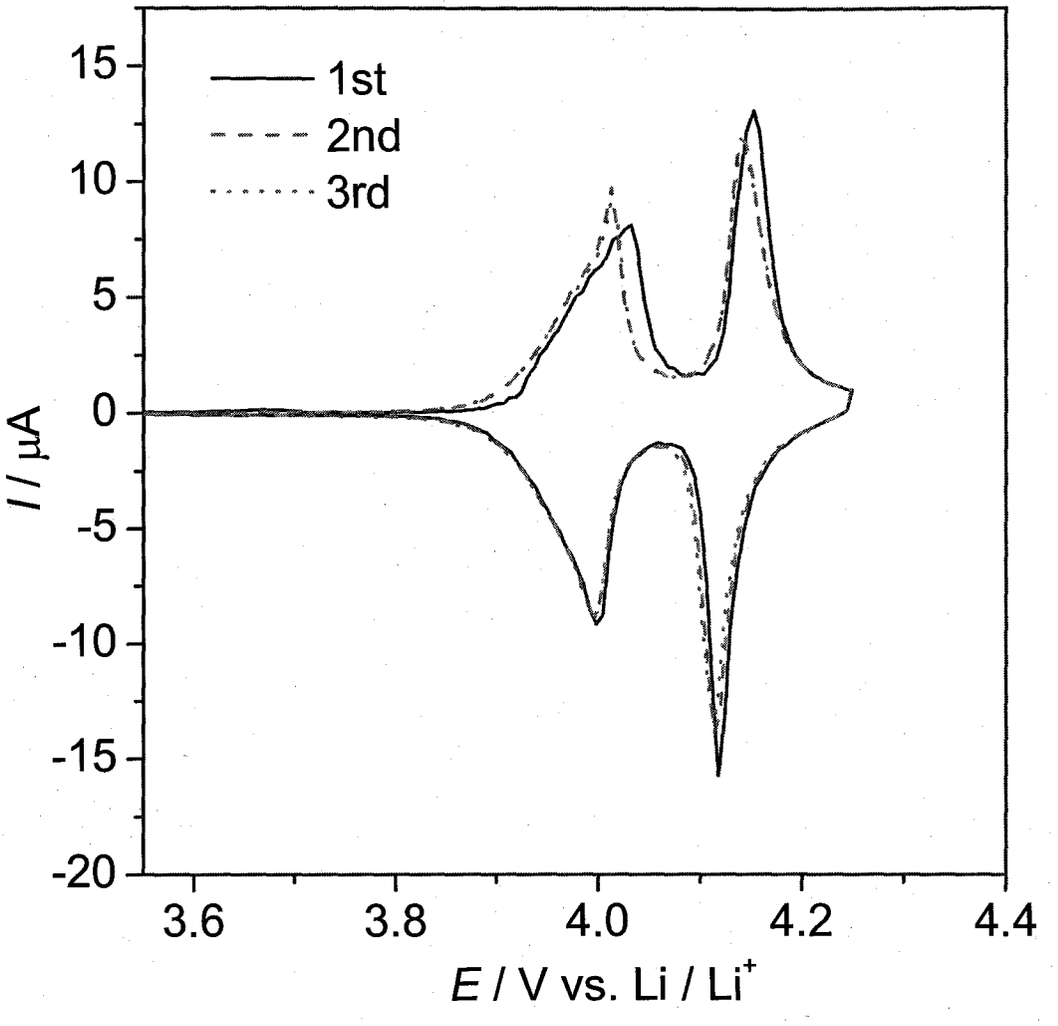

Fig. 1.2. Cyclic voltammogram of $LiMn_2O_4$ thin film electrode in 1mol dm^{-3} $LiClO_4$/PC. Scanning rate, 0.1 mV s^{-1}.

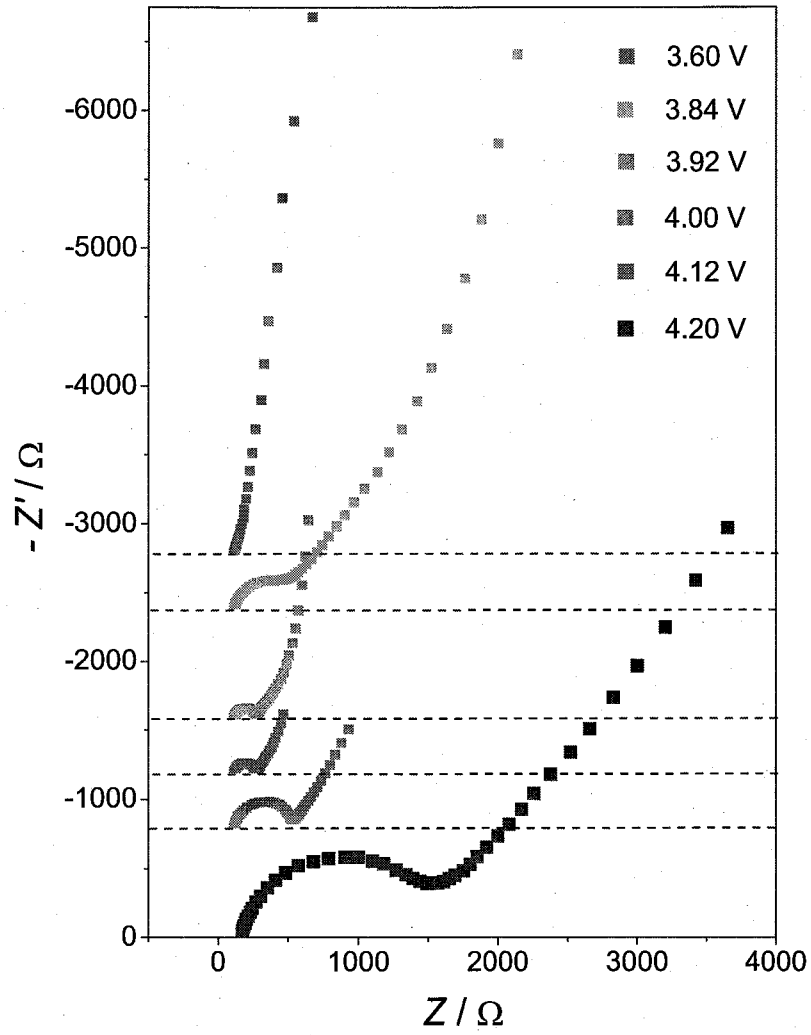

Fig. 1.3. Impedance spectra of $LiMn_2O_4$ thin film electrode in 1mol dm^{-3} $LiClO_4$/PC at potentials of 3.6, 3.84, 3.92, 4.0, 4.12 and 4.2 V.

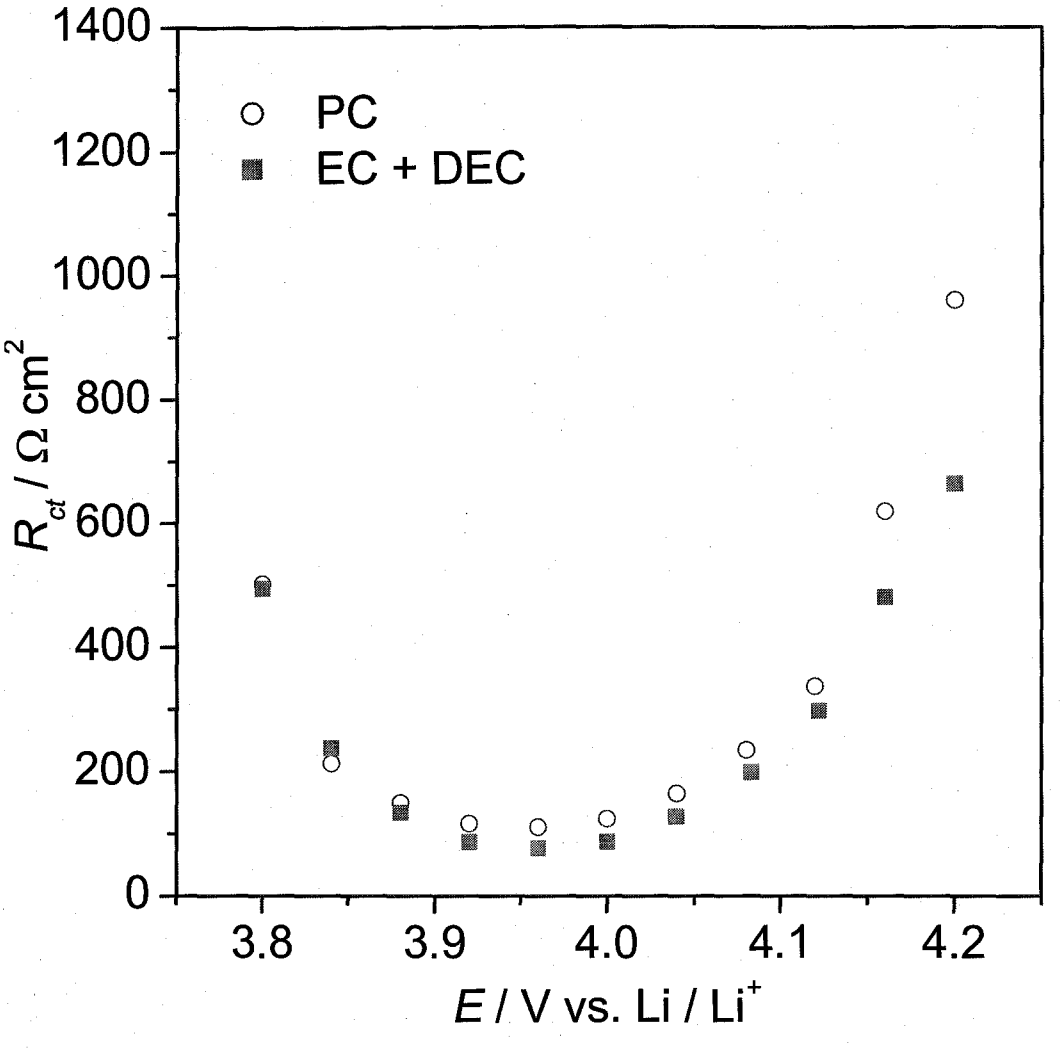

Fig. 1.4. Variation of charge (Li-ion) transfer resistances against electrode potentials. ○, 1mol dm^{-3} $LiClO_4$/PC; ■, 1 mol dm^{-3} $LiClO_4$/EC+DEC (1:1)

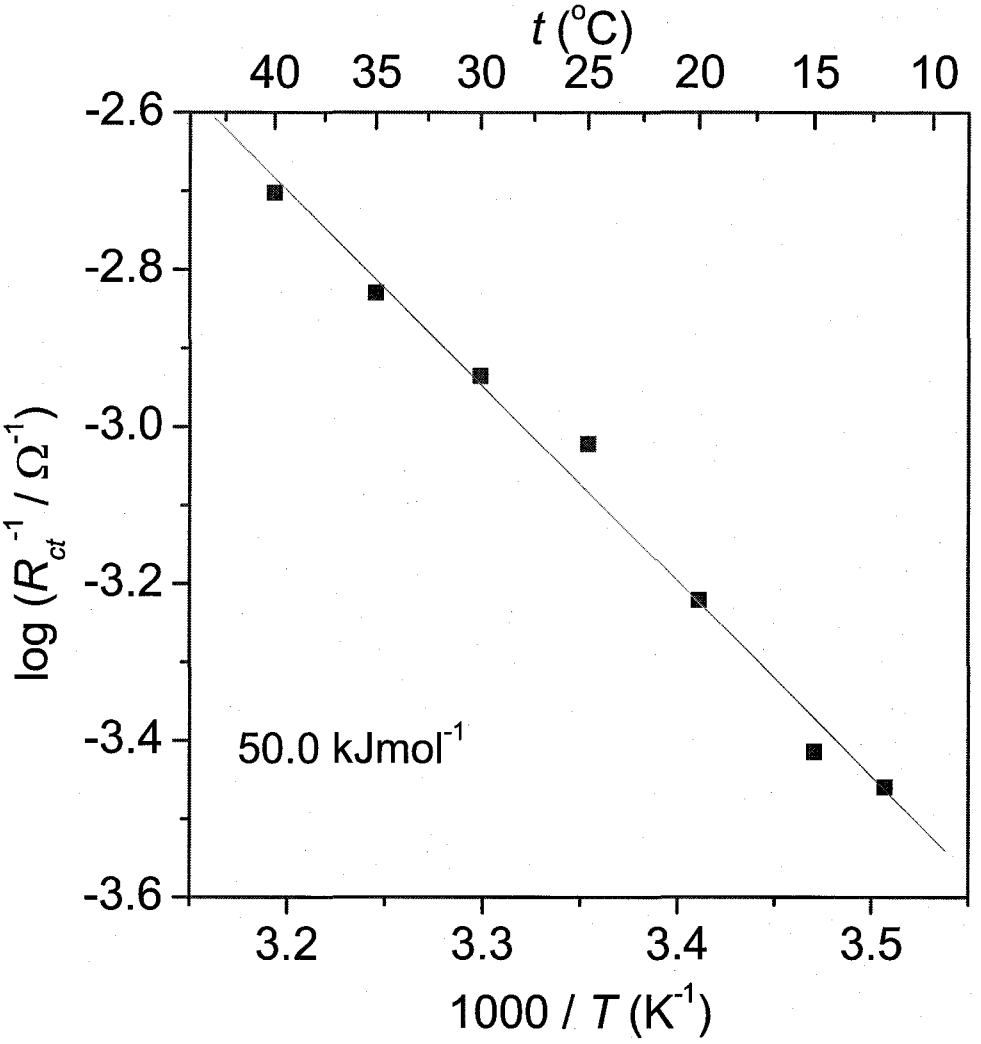

Fig. 1.5. Temperature dependency of charge (Li-ion) transfer resistances. Line is drawn by a least-squares method.

CHAPTER 2

Lithium-Ion Transfer at Positive Electrodes / Electrolyte Interface - Effect of Positive Materials -

2.1. Introduction

Due to the concerns of the lack of energy sources and environmental pollutions, secondary batteries, in particular Li-ion batteries have attracted much attention. Li-ion batteries have been used for portable electronic devices such as cellular phones, laptop personal computers, and others due to their high cell potential and large gravimetric density. Recently, they are expected as one of the candidates for power supply of electronic vehicles (EV) and hybrid electronic vehicles (HEV). While Li-ion batteries have played an important role on the trend of miniaturization of electronic devices, large-scale Li ion batteries for EV and HEV have been also developing.

One of the most important properties required for Li ion batteries in HEV is high rate performance, namely, fast charge and discharge reactions. Rate performances of Li-ion batteries are controlled by the reaction rate involved with Li-ion transfer. Therefore,

kinetics of Li-ion transfer in batteries should be well understood. Li-ion transfer in Li-ion batteries includes three different steps; Li-ion transfer across the interfaces between electrolyte / electrode, Li-ion diffusion through electrode and Li-ion transport through electrolytes. Latter two issues have been well investigated so far [1-5]. In addition to decrease the internal resistance of Li-ion batteries, diffusion path through active electrode material can be shortened by use of smaller size particles [6], and electrolyte resistances can be decreased by use of thinner electrolyte layer [7]. Then, the interfacial reaction should play very important role on the total rate of battery reactions. However, the interfacial Li-ion transfer has not been well understood yet.

For elucidation of interfacial Li-ion transfer at interface, structurally ordered interface of electrode is essential. The use of flat and homogeneous thin film electrode makes detailed study possible without considering the contributions of binder and conductive additives to electrochemical properties. In this paper, we have prepared $LiCoO_2$ thin films and $LiMn_2O_4$ thin films by pulsed laser deposition, and then Li-ion transfer at electrode / electrolyte interface was studied.

2.2. Experimental

Positive thin film electrodes of $LiCoO_2$ and $LiMn_2O_4$ were prepared by pulsed laser ablation using KrF eximer laser of a wavelength of 248 nm (Japan Storage Battery, EXL-210) with polished Pt plate as a substrate. During deposition, a substrate was kept at 873 K for $LiCoO_2$ and 973 K for $LiMn_2O_4$. Detailed deposition conditions were reported elsewhere [8, 9]. Prepared thin films were characterized by X-ray diffraction (XRD) measurement using Rint-2500 (Rigaku) equipped with a graphite monochromator and a scintillation detector. Measurement conditions were 40 kV and 250 mA with a scanning speed of 0.125 s. Electrochemical properties of $LiCoO_2$ and $LiMn_2O_4$ thin film electrode were studied by cyclic voltammetry with the use of a three-electrode electrochemical cell by HSV-100 (HOKUTO DENKO Inc.). Lithium metal was used as reference and counter electrodes and thin film electrode as a working electrode. Unless otherwise mentioned,

potentials are referred to Li metal. Electrolyte used was propylene carbonate (PC) containing 1 mol dm^{-3} lithium perchlorate.

Li-ion transfer at positive thin film electrode was studied by AC impedance spectroscopy using Radiometer (Voltalab 40) over the frequency range from 100 kHz to 10 mHz with the same three-electrode electrochemical cell.

All experiments were conducted under Ar atmosphere.

2.3. Results and discussion

2.3.1. Characterization of $LiCoO_2$

Figure 1 shows XRD pattern of a $LiCoO_2$ thin film deposited on Pt plate at 873 K for 1h. Number on peaks denotes index *hkl*. Except for substrate peaks, only one peak 2θ= 18.95 is remarkable indexed as the reflection of 003 plane of hexagonal $LiCoO_2$. The result shows that the $LiCoO_2$ thin film had a preferred c-axis orientation to the substrate surface.

Electrochemical behavior of $LiCoO_2$ thin film was examined by cyclic voltammetry in 1 mol dm^{-3} $LiClO_4$ / PC. As is shown in Figure 2, a large peak at 3.92 V and very small peaks at 4.08 V and 4.18 V appeared in cathodic direction. These peaks correspond to phase transitions of $LiCoO_2$ [10]. These results showed resultant $LiCoO_2$ thin films showed almost similar electrochemical properties with $LiCoO_2$ so far reported in literature [10]. The peak separation of the redox couple in figure 2 was about 40 mV. This small peak separation means that the ohmic drop is small and therefore the electric conductivity of the $LiCoO_2$ thin film is high enough for electrochemical measurements.

2.3.2. Characterization of $LiMn_2O_4$

Figure 3 shows XRD pattern of a $LiMn_2O_4$ thin film deposited on Pt substrate [11]. Several peaks were observed at 2θ= 18.5, 36.0, 38.0, 43.7, 57.8, 63.9, indexed as 111, 311, 222, 400, 511, 440 respectively [12]. This XRD pattern indicates that single-phase spinel

$LiMn_2O_4$ was obtained. Very sharp peaks demonstrate the resultant $LiMn_2O_4$ thin film is well crystallized.

Redox behavior of $LiMn_2O_4$ thin film electrode was examined by cyclic voltammetry in 1 mol dm^{-3} $LiClO_4$ / PC. As is shown Fig.4, two couples of redox peaks were observed at 4.0 V and 4.1 V. The peak separation was about 30 mV, indicating that the ohmic drop is very small as is also mentioned above and therefore the electric conductivity of the $LiMn_2O_4$ thin film electrode can be considered to be high enough for electrochemical measurements.

2.3.3. AC impedance spectroscopy

AC impedance measurements were carried out at thin film electrode / electrolyte interface. In figure 5 are shown Nyquist plots at given potentials ranging 3.7-4.2 V. At potential below 3.7 V, no semi-circle but only blocking electrode behavior appeared. Little oxidation and reduction currents were observed in cyclic voltammogram in figure 2 below 3.7 V, and therefore blocking electrode behaviors are very quite valid because few Li^+ ions are inserted or extracted. At potentials above 3.92 V, one semi-circle appeared in the higher frequency region followed by a diffusional behavior in the lower frequency region. Resistances evaluated from semi-circle are dependent on electrode potentials and also on the salt concentration of electrolyte used, indicating that the process responsible for the observed semi-circle is closely related with the relaxation process of Li-ion. Hence, it is reasonable to consider that the resistance is ascribed to the Li-ion (charge) transfer at interface.

Similarly to $LiCoO_2$ thin film electrode / electrolyte interface, AC impedance measurements were conducted on $LiMn_2O_4$ thin film electrode. In figure 6, Nyquist plots are shown at given potentials ranging 3.6-4.2 V. At electrode potential of 3.6 V, no semi-circle appeared and blocking-electrode-type behavior was observed, indicating no lithium ion insertion and extraction occur in $LiMn_2O_4$ thin film electrode. This phenomenon is proved by the cyclic voltammogram given in Fig.4, in which no oxidation and reduction currents were observed at 3.6 V. At potentials above 3.84 V, one semi-circle

in the frequency region and linear line in the lower frequency appeared. Resistances evaluated from semi-circles are dependent on electrode potentials, indicating that the impedance should be ascribed to the resistances of interfacial Li-ion transfer.

2.3.4. Li ion transfer resistances

As is described before, one semi-circle in the Nyquist plots should be ascribed to Li-ion transfer resistances. Figure 7 shows the Li-ion transfer resistances against electrode potentials in 1 mol dm^{-3} $LiClO_4$ / PC of $LiCoO_2$ thin film (open circles) and $LiMn_2O_4$ thin film (closed squares). Li-ion transfer resistance exhibited different dependency on electrode potentials. For $LiCoO_2$ thin film electrode, Li-ion transfer resistance appeared at around 3.9 V and the resistance decreased with increasing electrode potential up to 4.2 V. On the other hand, Li ion transfer resistance on $LiMn_2O_4$ appeared around 3.8 V and decreased with increasing electrode potential up to 4.0 V and then increased with increasing electrode potential. These behaviors can be explained as follows; Charge (lithium-ion) transfer resistance (R_{ct}) is expressed by this formula. $i_O = RT/nFAR_{ct}$ (i_O : exchange current, R : gas constant, T : temperature, n : stoichiometric number of electrons involved in the electrode reaction, F : Faraday constant, A : area) [13]. As shown in cyclic voltammograms of figures 2 and 4, Li-ion insertion and extraction occurs at about 3.9 V for $LiCoO_2$ and 3.8 V for $LiMn_2O_4$. Therefore, it is very reasonable that the Li-ion transfer resistances appeared at these potentials as given in figure 7. Above these electrode potentials, Li-ion insertion and extraction reaction proceed, leading to the increase of exchange currents, resulting in the decrease of charge transfer resistances with the increase of electrode potentials at early stage. At the next stage, charge transfer resistances are kept almost constant to some degree and then increase again with increasing electrode potentials. The increase of charge transfer resistances can be explained by two factors. One is the decrease of Li-ion site in positive electrode materials. At higher electrode potentials, the number of available sites for Li-ion decreases and therefore exchange currents should become small. The other is the decomposition of electrolytes. At higher potentials, electrolyte decomposition may take place and some kind of passivation film may be

formed on positive thin film electrode [14]. This passivation film may retard the Li-ion kinetics at electrode or decrease the active sites for Li-ion to insert and extract. In fact, charge transfer resistances were not decreased again when electrode potential was decreased from 4.2 V to negative potentials. This result indicates that some irreversible phenomena should occur. These two factors lead to the increase of charge transfer resistances at higher potential.

It should be noted that minimum values of Li-ion transfer resistance are very different by positive electrode materials. At 4.0 V, the value of resistance on $LiMn_2O_4$ thin film electrode was 150 ohm; while that of $LiCoO_2$ was 500 ohm, which is four times larger than that of $LiMn_2O_4$. Since the reactive surface areas are regulated to be the same by o-ring, this large difference should be caused by electrodes themselves. As described above, $LiCoO_2$ has a layer-typed 2 dimensional structure. On the other hand, $LiMn_2O_4$ has a spinel-typed 3 dimensional structure. Li-ion inserts and extracts at the reactive sites of the interface. The effective area of $LiCoO_2$ for Li-ion insertion and extraction is restricted to the only defects of layers because of their preferential *c*-axis orientation of $LiCoO_2$ thin film. In contrast, $LiMn_2O_4$ has 3D structure and many sites for Li-ion insertion and extraction would exist on the surface of $LiMn_2O_4$ thin film electrode. Therefore, the large difference of charge transfer resistance should be the number of sites at the electrode / electrolyte interface.

Figure 8 shows the Li-ion transfer resistances of $LiCoO_2$ thin film electrode against electrode potentials as cycled. In charging direction, Li ion transfer resistances decreased with increasing electrode potentials and then kept constant with increasing electrode potential. On the other hand in discharging direction, Li-ion transfer resistances increased with decreasing electrode potentials. Although this tendency remained unchanged, the absolute value of resistances was increased with cycles. As mentioned above, irreversible reaction occurred and passivation film should be formed on $LiCoO_2$ thin film electrode at higher electrode potential to increase Li-ion transfer resistances.

In figure 9, the Li-ion transfer resistances of $LiMn_2O_4$ thin film against electrode potentials as cycled are shown. The behaviors of Li-ion transfer resistances were almost the same in charge and discharge direction expect for the first charge. Differently from the

case of $LiCoO_2$, Li-ion transfer resistances decreased with decreasing electrode potentials, and the absolute value of resistances did not increased remarkably. This result indicates reversible reaction should occur at higher electrode potential on $LiMn_2O_4$ thin film electrode.

Different behaviors were observed for $LiCoO_2$ and $LiMn_2O_4$ thin film electrodes as cycled in terms of reversibility at higher electrode potentials. The irreversible behavior should be ascribed to the electrolyte decomposition. Electrolyte decomposition may be catalytically promoted by transition metals of positive electrode materials, and therefore the different behavior of charge transfer resistances as cycled for $LiCoO_2$ and $LiMn_2O_4$ thin film electros, should take place.

Activation barrier at electrode / electrolyte interface for Li-ion transfer was studied. Figure 10 shows temperature dependency of Li-ion transfer resistances of $LiCoO_2$ (open circles) and $LiMn_2O_4$ (closed squares) in 1mol dm^{-3} $LiClO_4$ / PC. By the least-squares method, apparent activation energies for Li ion transfer resistances were determined to be 46 ± 7.3 $kJmol^{-1}$ for $LiCoO_2$ at 4.10 V and 50 ± 2.4 $kJmol^{-1}$ at 3.94 V for $LiMn_2O_4$. Although the active materials are different, the values of apparent activation energies are similar irrespective with positive electrode materials. These values are very large as compared with those for Li-ion diffusion through active materials and Li-ion transport through liquid electrolytes [1, 15]. Thus, these results indicate that a high activation barrier exists at the interface between positive electrode / electrolyte. Our recent studies for the large activation barriers at interface between electrode / electrolyte revealed that the de-solvation is responsible for the activation energies [16-18]. Therefore, the present results seem to be quite valid.

2.4. Conclusions

Li-ion transfer at positive electrode / electrolyte was studied using structurally ordered interface consisting of $LiCoO_2$ and $LiMn_2O_4$ thin film electrodes / electrolyte. Li-ion transfer resistances were influenced by structures of positive materials. As cycled,

irreversible behavior took place for $LiCoO_2$ while Li-ion transfer resistances for $LiMn_2O_4$ showed the reversible behavior. Large activation barriers at positive electrode / electrolyte interface become clear. Based on the present studies, the rate performance can be enhanced by the control of electrode / electrolyte interface, in particular when layered active materials are used in Li-ion batteries.

References

[1] A. Van der Ven and G. Ceder, *Electrochem. Solid. State. Lett.,* **3**(2000), 301

[2] D. Aurbach, K. Gamolsky, B. Markovsky, G. Salitra, Y. Gofer, U. Heider, R. Oesten and M. Schmidt, *J. Electrochem. Soc.,* **147**(2000),1322

[3] A. Funabiki, M. Inaba, Z. Ogumi, S. Yuasa, J. Otsuji and A. Tasaka, *J. Electrochem., Soc.* **145**(1998), 172

[4] A. Ferrya, G. Oradd and P. Jacobsson, *J. Chem. Phys.,* **108**(1998), 7426

[5] B. Klassen, R. Aroca, M. Nazri and G.A. Nazri, *J. Phys. Chem. B,* **102**(1998), 4795

[6] J.B. Bates, N.J. Dudney, B. Neudecker, A. Ueda and C.D. Evans, *Solid. State. Ionics.,* **135**(2000), 33

[7] B.J. Neudecker, N.J. Dudney and J.B. Bates, *J. Electrochem. Soc.,* **147**(2000), 517

[8] Y. Iriyama, M. Inaba, T. Abe and Z. Ogumi, *J. Power Sources.,* **94**(2001), 175

[9] M. Inaba, T. Doi, Y. Iriyama, T. Abe and Z. Ogumi, *J. Power Sources.,* **81-82**(1999), 554

[10] J.N. Reimers and J.R. Dahn, *J. Electrochem. Soc.,* **139**(1992), 2091

[11] I. Yamada, T. Abe, Y. Iriryama and Z. Ogumi, *Electrochem. Comm.,* **5**(2003), 502

[12] *JCPDS No35-0782*

[13] A. J. Bard and L. R. Faulkner, *Electrochemical Methods, Fundamental and Applications, second edition.*,John Wiley & Sons,Inc, New York, 2000, pp. 115.

[14] D. Aurbach, *J. Power Sources.,* **89**(2000), 206

[15] G. Kumar, Janaklraman, N. Namboodlrl, Gangadharan, KanagaraJ, Saminathan and N. Sharlef, *J. Chem. Eng. Data.,* **36**(1991), 467

[16] T. Abe, H. Fukuda, Y. Iriyama and Z. Ogumi, *J. Electrochem. Soc.,* **151**(2004), A1120

[17] F. Sagane, T. Abe, Y. Iriyama and Z. Ogumi, *J. Power Sources.,* **146**(2005), 749

[18] T. Doi, K. Miyatake, Y. Iriyama, T. Abe, Z. Ogumi and T. Nishizawa, *Carbon* **42**(2004), 3183

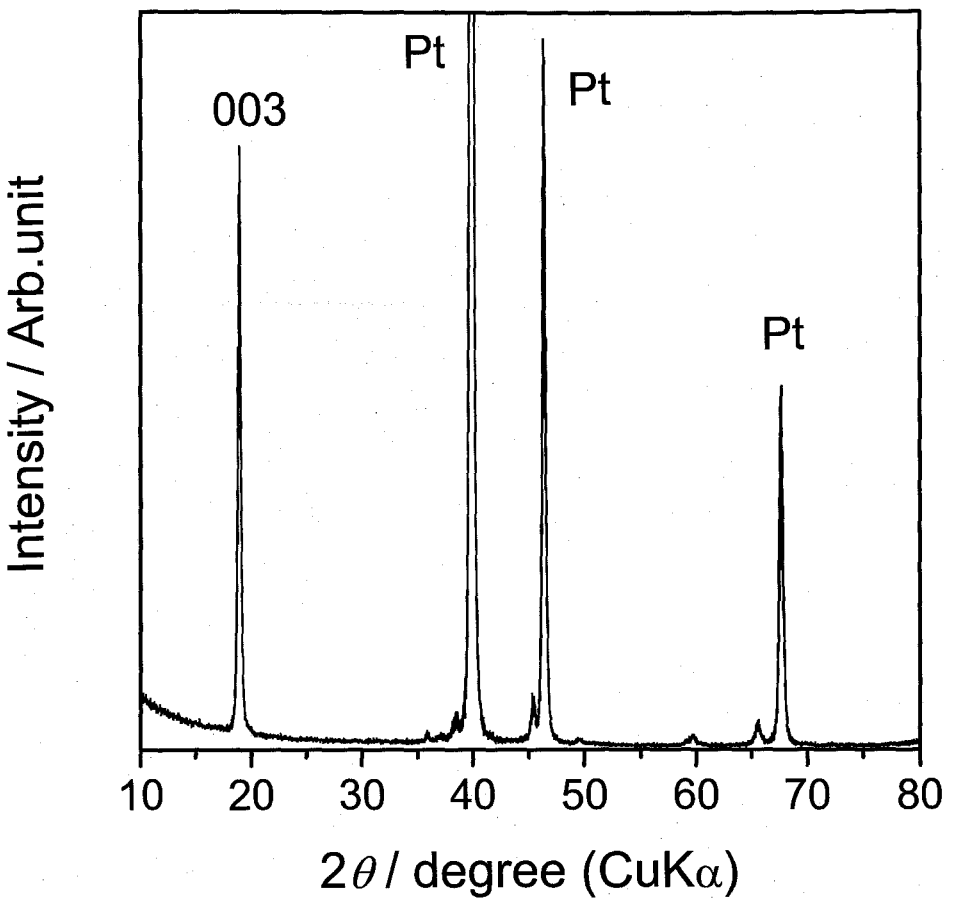

Fig 2.1. X-ray diffraction pattern of $LiCoO_2$ thin film on Pt plate. Number on peaks denotes index *hkl*.

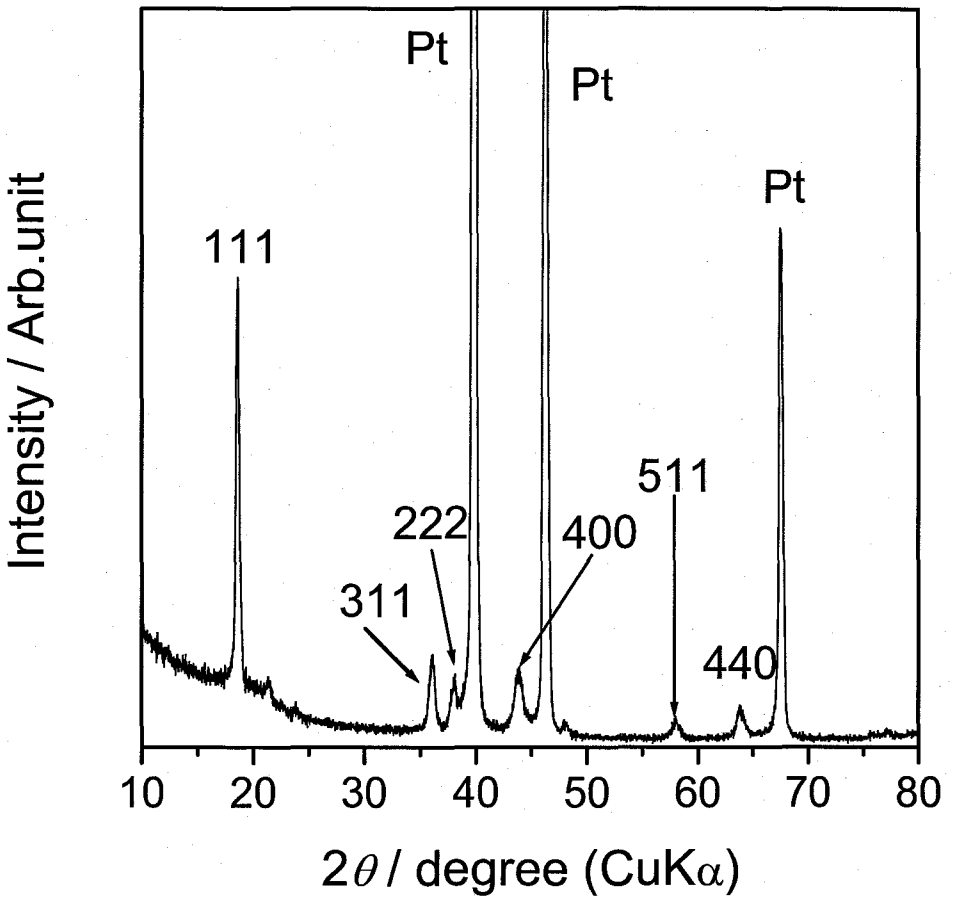

Fig 2.2. X-ray diffraction pattern of $LiMn_2O_4$ thin film on Pt plate. Number on peaks denotes index *hkl*.

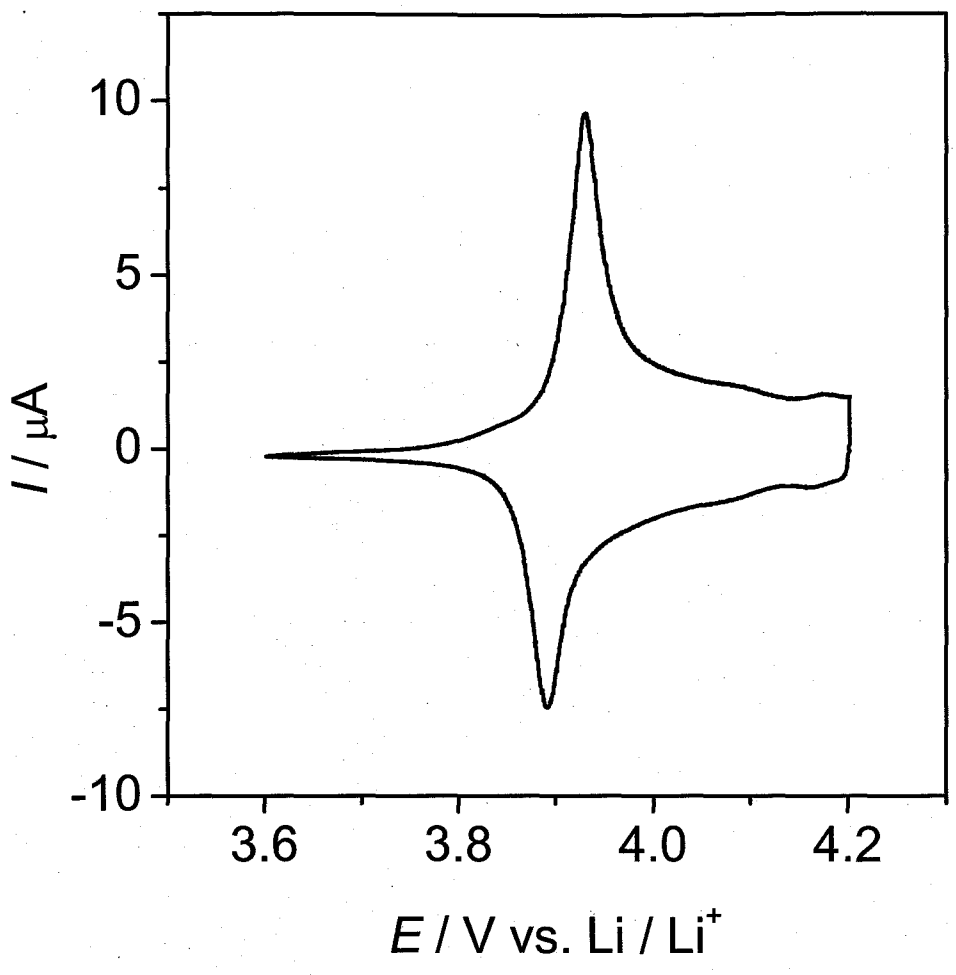

Fig 2.3. Cyclic voltammogram of $LiCoO_2$ thin film electrode in 1 mol dm_{-3} $LiClO_4$ / PC. Scanning rate is 0.1 mV s^{-1}.

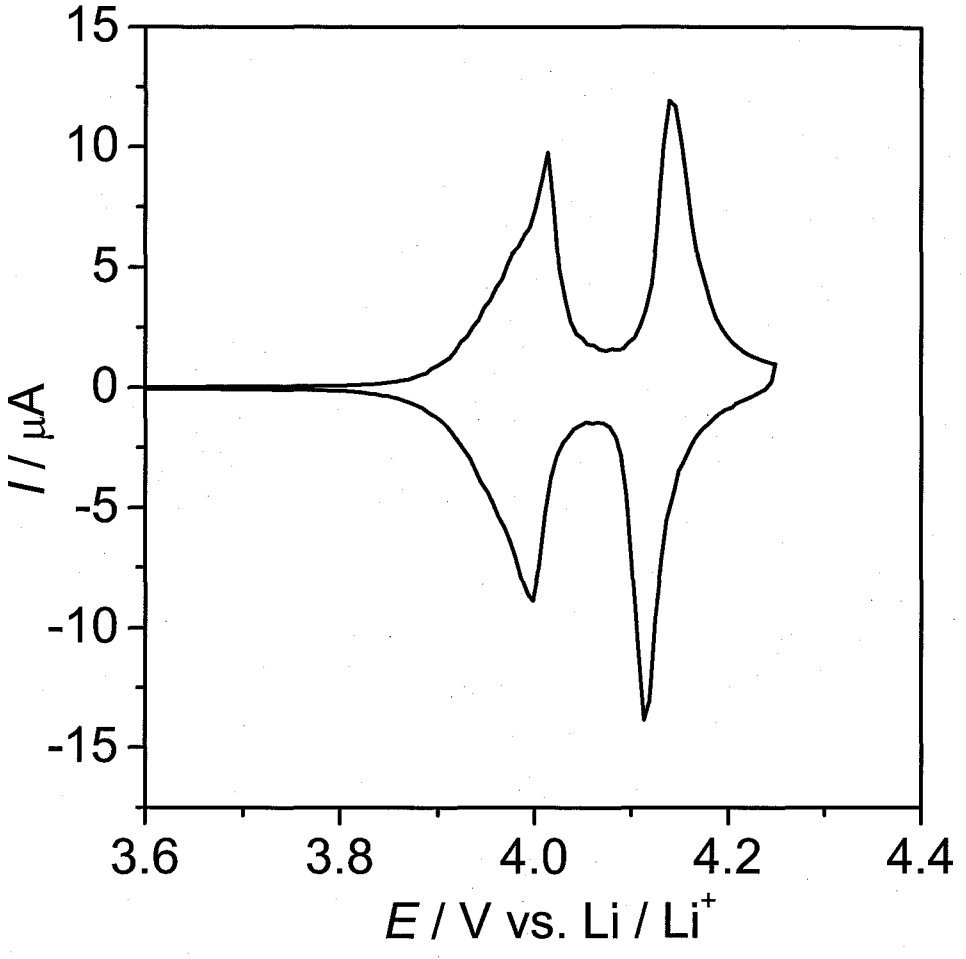

Fig 2.4. Cyclic voltammogram of $LiMn_2O_4$ thin film electrode in 1 mol dm_{-3} $LiClO_4$ / PC. Scanning rate is 0.1 mV s^{-1}.

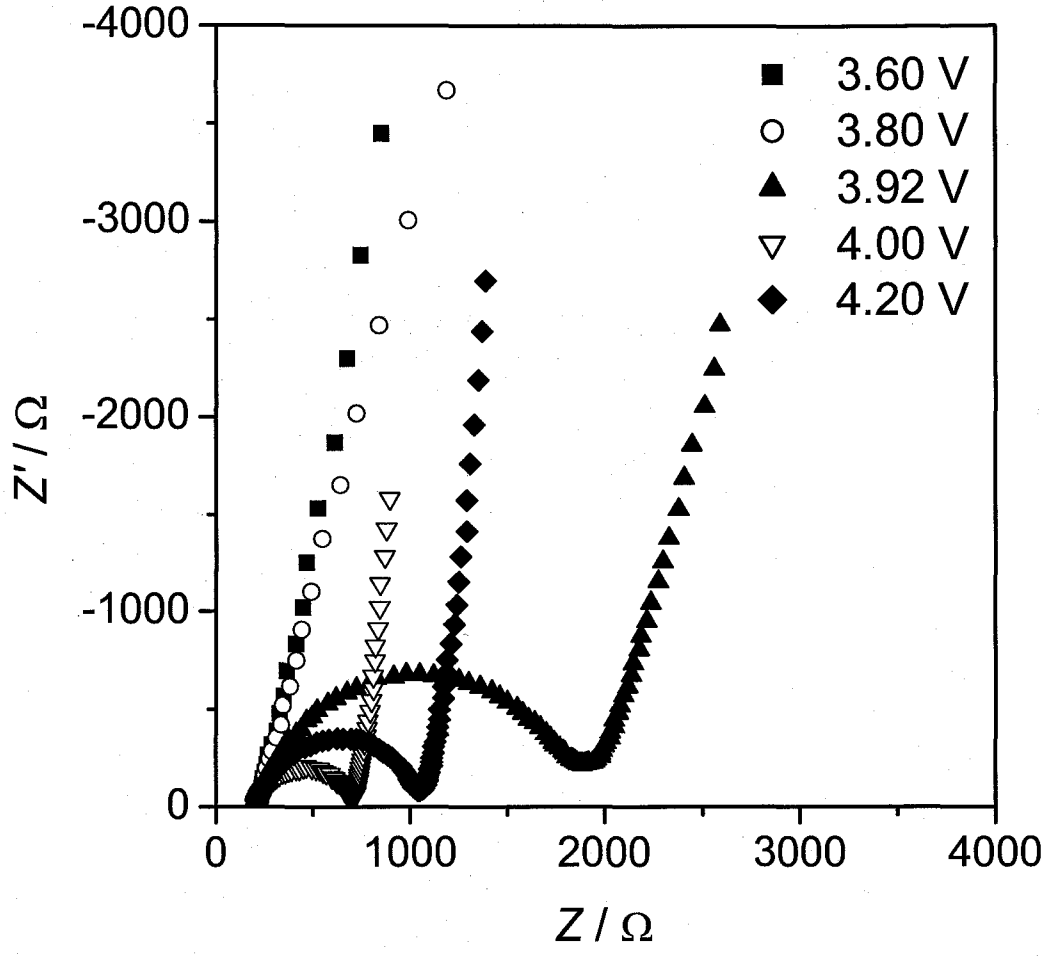

Fig 2.5. Impedance spectra of $LiCoO_2$ thin film electrode in 1 mol dm^{-3} $LiClO_4$ / PC at potentials of 3.60, 3.80, 3.92, 4.00, and 4.20 V.

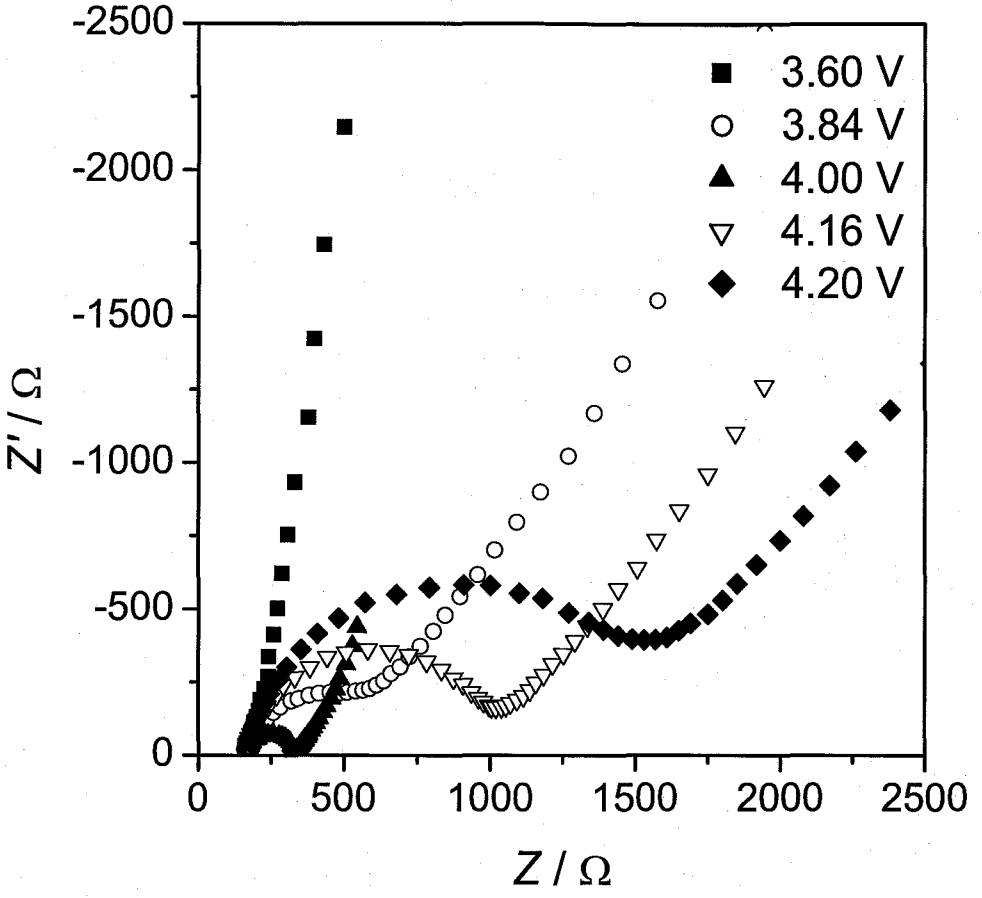

Fig 2.6. Impedance spectra of $LiMn_2O_4$ thin film electrode in 1 mol dm^{-3} $LiClO_4$ / PC at potentials of 3.60, 3.84, 4.00, 4.16 V and 4.20 V.

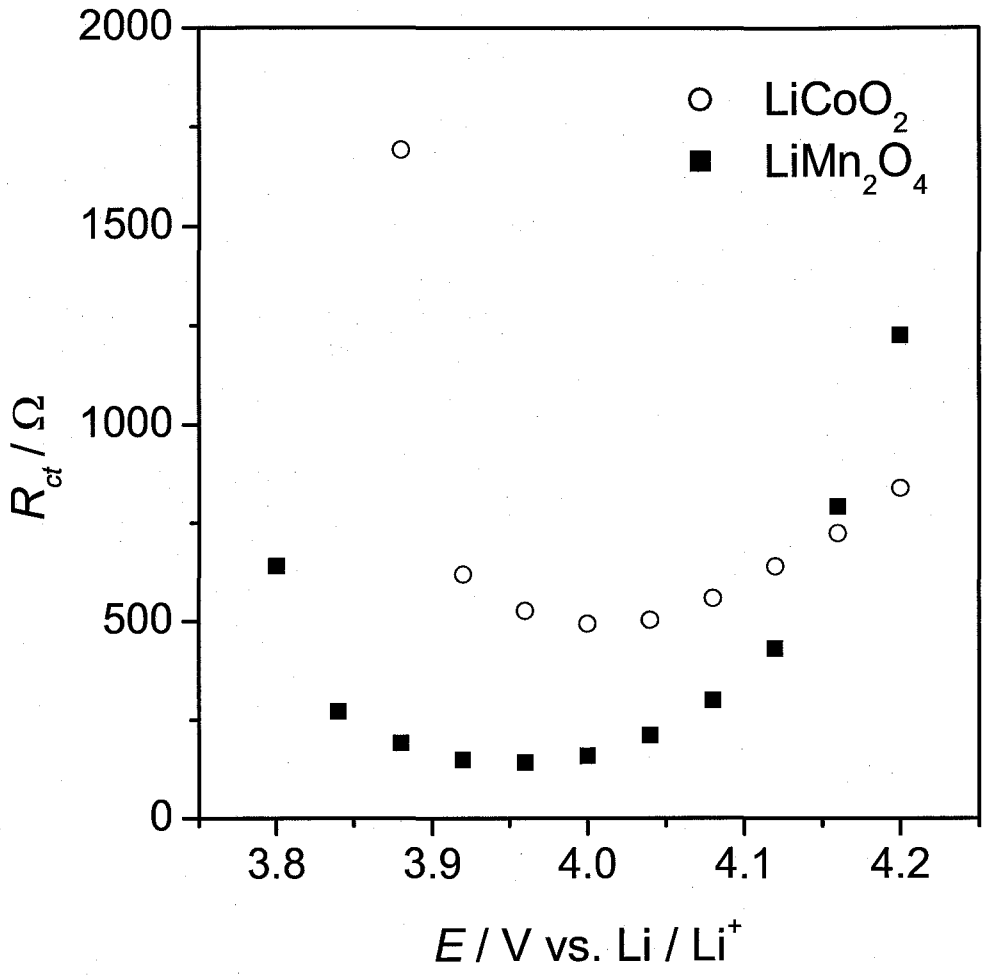

Fig 2.7. Variation of charge transfer resistances against electrode potentials. ○, $LiCoO_2$, ■, $LiMn_2O_4$.

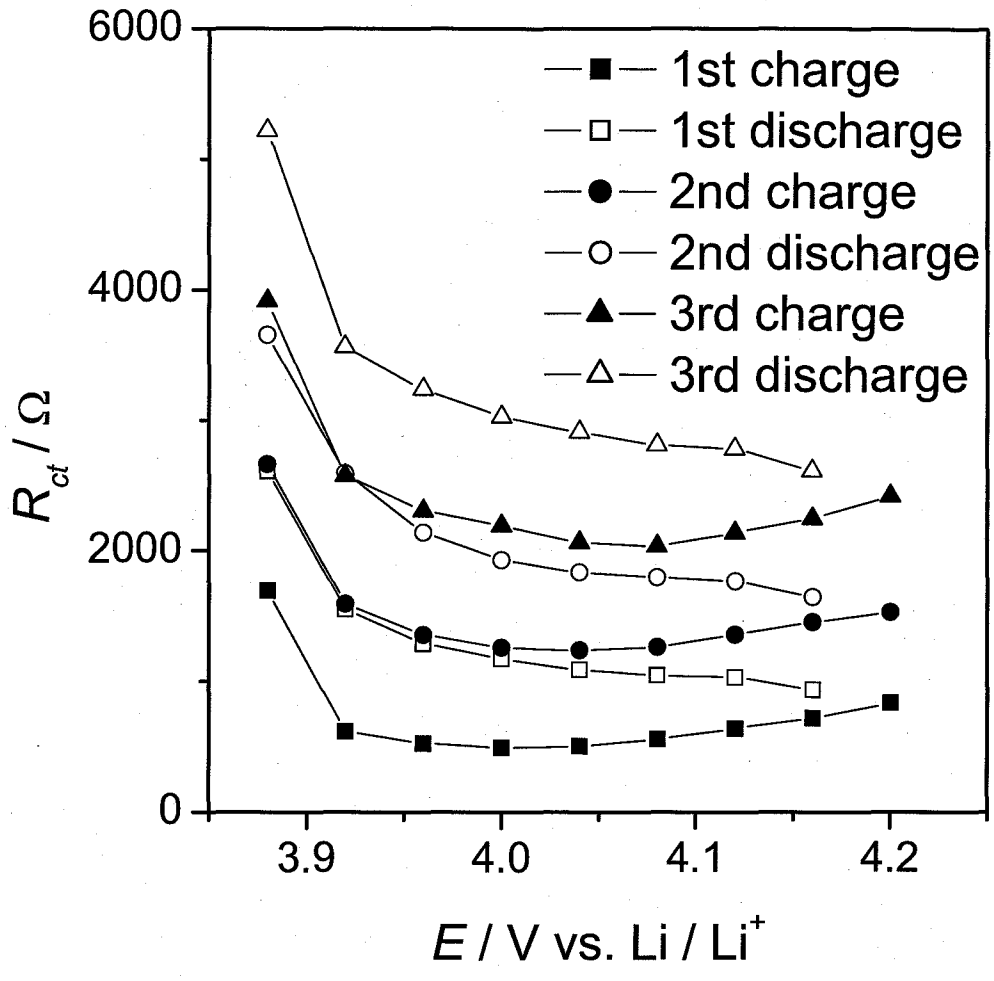

Fig 2.8. Variation of charge transfer resistances on $LiCoO_2$ thin film electrode against electrode potentials as cycles.

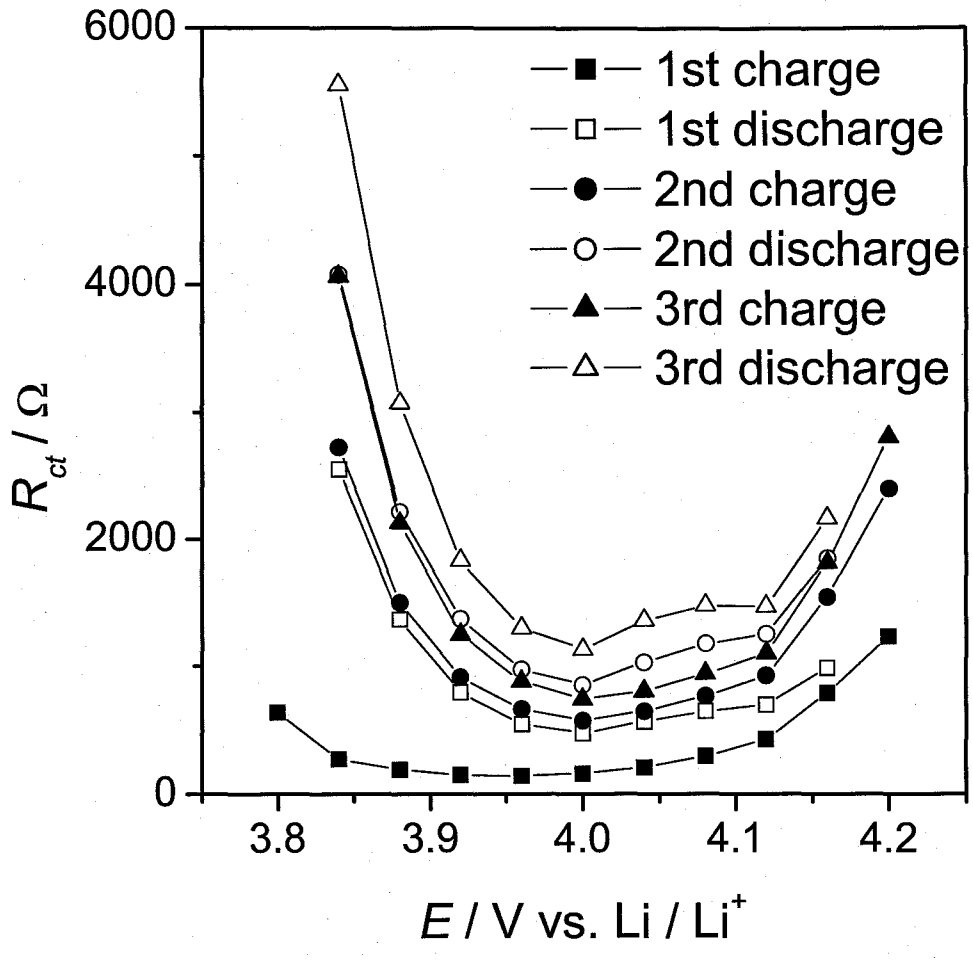

Fig 2.9. Variation of charge transfer resistances on $LiMn_2O_4$ thin film electrode against electrode potentials as cycles.

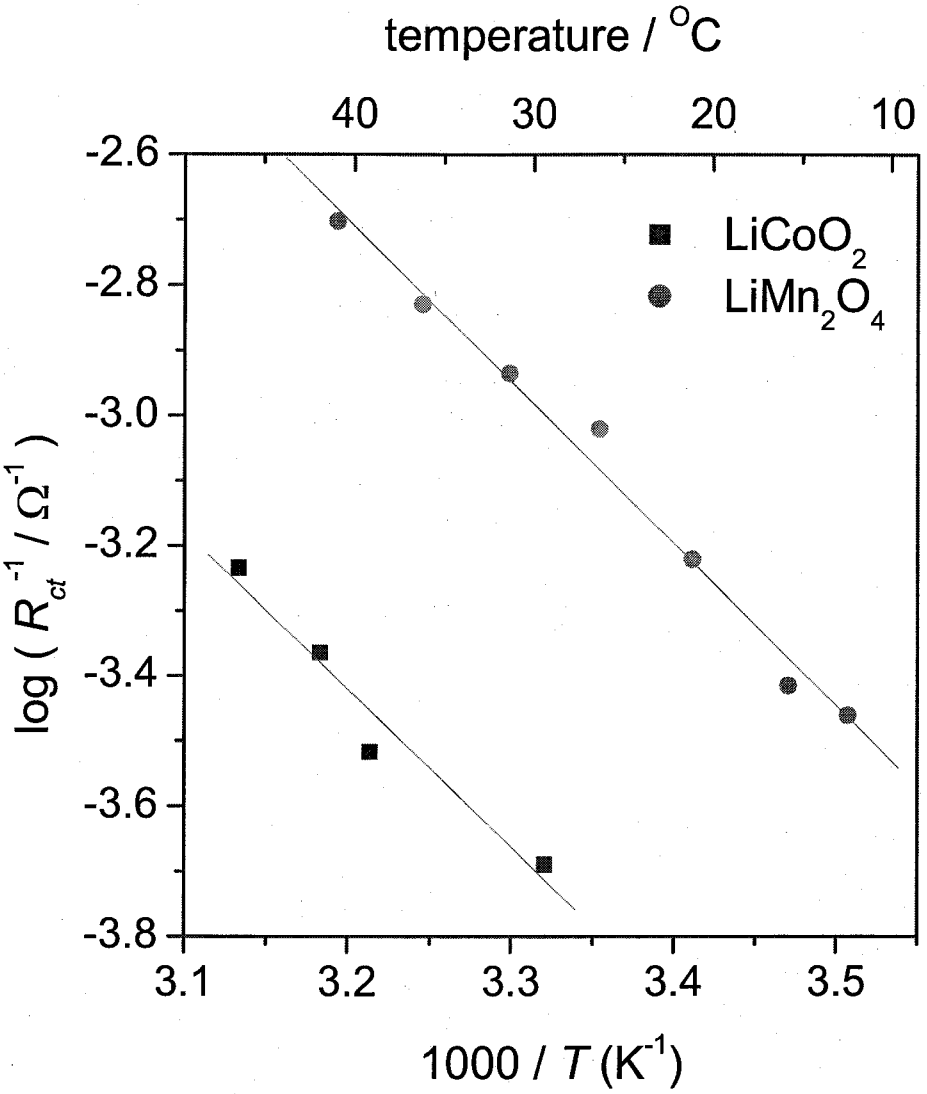

Fig 2.10. Temperature dependence of charge transfer resistances of positive thin film / electrolyte interface. ■,$LiCoO_2$, ●,$LiMn_2O_4$. Line is drawn by a least-squares method.

CHAPTER 3

Lithium-Ion Transfer on a Li_xCoO_2 Thin Film Electrode Prepared by Pulsed Laser Deposition - Effect of Orientation -

3.1. Introduction

The increase in worldwide energy consumption has led to the depletion of natural resources and an increased environmental burden, which are urgent problems to be solved. One practical approach to increased energy consumption is to increase the utilization efficiency. In this sense, secondary batteries have attracted much attention since hybrid electric vehicles (HEV) that use nickel hydrogen batteries show dramatic increase in gas mileage. Recently, Li-ion batteries have attracted much attention as power sources for next-generation EV and HEV.

If they are to be used as power sources for EV and HEV, fast charge and discharge reactions are required. Therefore, the internal resistance in Li-ion batteries should be decreased as much as possible. In Li-ion batteries, the charge and discharge reactions are based on Li-ion transfer between the positive and negative electrodes through an electrolyte. In this reaction, three Li-ion transfer processes should be considered: Li-ion

diffusion through the electrode materials, Li-ion (solvated Li-ion) transport and migration in the electrolyte, and Li-ion transfer at the electrode / electrolyte interface. To attain fast charging and discharging, the reaction rates in these processes must be increased. Among these processes, the former two can be made faster by shortening the diffusion and migration paths using thinner electrode and electrolyte layers [1]. The use of fine active materials can also be used to decrease the diffusion path of Li-ion and to increase the number of reaction sites for Li-ion to insert and extract [2]. Li-ion transfer at the interface also plays an important role in the total rate of the battery reaction. However, this important process of Li-ion transfer at the interface is not yet well understood. Elucidation of the fundamental mechanism of Li-ion transfer at the interface should be important for the further development of higher-performances Li-ion batteries.

A detailed study of Li-ion transfer at the interface requires a structurally ordered interface consisting of pure active materials without any additives. In this study, we prepared $LiCoO_2$ thin films with different orientations by pulsed laser deposition, and then examined Li-ion transfer at the electrode / electrolyte interface.

3.2. Experimental

Positive thin film electrodes of $LiCoO_2$ with different orientations were prepared by pulsed laser deposition using a KrF eximer laser with a wavelength of 248 nm (Japan Storage Battery, EXL-210), with polished Pt plates as substrates. The substrate was kept at 873 K under a stream of oxygen. $LiCoO_2$ thin films with different orientations were prepared by changing the deposition time (range 1 h to 3 h). The resulting $LiCoO_2$ thin films were characterized by X-ray diffraction (XRD) and Raman spectroscopy. XRD was measured with a RINT-2200 (Rigaku) equipped with a graphite monochromator with a scintillation detector. Typical working conditions were 40 kV and 40 mA with a scanning speed of 1 s. Raman spectroscopy was conducted with a triple monochromator (Jobin-Yvon, T-64000) with a multi-channel charge-coupled device (CCD) detector. A 515.4-nm line (50 mW) from an argon ion laser (NEC, GLG3280) was used as a light

source.

The electrochemical properties of $LiCoO_2$ thin film electrodes were studied by cyclic voltammetry with a three-electrode cell that used lithium metal as counter and reference electrodes (HSV-100, HOKUTO-DENKO Inc.). Unless otherwise stated, potentials are referenced to lithium metal. The electrolytes used were propylene carbonate (PC) containing 1 mol dm^{-3} $LiClO_4$ or 1 mol dm^{-3} $LiCF_3SO_3$.

Interfacial reactions between the electrode and electrolyte were studied by AC impedance spectroscopy using a Radiometer (VoltaLab40) over a frequency range of 100 kHz to 10 mHz with the same three-electrode cell.

All experiments were conducted under an Ar atmosphere.

3.3. Results and Discussion

3.3.1. Structural characterization of $LiCoO_2$ thin films

Figures 1(a) and 1(b) show XRD patterns of $LiCoO_2$ thin films deposited on a Pt plate for 1 and 3 h, respectively. Numbers on peaks denote the index *hkl*. As shown in Fig.1 (a), only one peak 2 = 19.0 is remarkable, other than peaks due to the substrate. This peak can be indexed as the reflection of the 003 plane of hexagonal $LiCoO_2$, indicating that the thin film deposited for 1 h is a *c*-axis-oriented film. In contrast, several peaks were observed for the film deposited for 3 h, as shown in Fig.1 (b). In addition to 003, peaks indexed as the reflections of the 104, 015, 107, and 018 planes of hexagonal $LiCoO_2$ were also seen. The peak intensities of 003 and 104 were almost the same. Hence, the film deposited for 3 h should possess a random orientation.

Considering interface between $LiCoO_2$ thin films and the electrolyte, c-axis-oriented thin film deposited for 1 h has very few sites of Li ion transfer at defects on the surface and planes other than 003. On the other hand, the random thin film deposited for 3 h has more sites because the Li-ion layer faces the interface vertically.

Raman spectroscopy measurements were also carried out. Figure 2 shows Raman

spectra of $LiCoO_2$ thin films deposited for (a) 1 h and (b) 3 h. Stoichiometric $LiCoO_2$ shows two Raman bands at 486 cm^{-1} (E_g mode) and 596 cm^{-1} (A_{1g} mode) [3]. As shown in Fig. 2, both E_g and A_{1g} peaks were observed in each thin film. In addition to the E_g and A_{1g} peaks, a small peak was observed at 690 cm^{-1}, which was assigned to Co_3O_4. Figure 2 (a) and (b) showed similar spectra. However, the ratio of the peak intensity of E_g to that of A_{1g} varies with a change in the degree of *c*-axis-orientation of $LiCoO_2$ thin films [4].

3.3.2. Electrochemical properties of $LiCoO_2$ thin films

The electrochemical properties of $LiCoO_2$ thin film electrodes were examined in liquid electrolyte of 1 mol dm^{-3} $LiClO_4$ / PC. Figure 3 shows cyclic voltammograms of the *c*-axis-oriented $LiCoO_2$ thin film deposited for 1 h. A large peak at 3.92 V and very small peaks at 4.08V and 4.18 V appeared in the cathodic direction. These peaks correspond to the phase transition of $LiCoO_2$, suggesting that the resultant $LiCoO_2$ thin film showed electrochemical properties almost identical to those in the literature [5]. The peak separation of the redox couple at around 3.9 V was about 40 mV, which suggests a small ohmic drop, and therefore the electric conductivity of the *c*-axis-oriented $LiCoO_2$ thin film is high enough for electrochemical measurements.

Figure 4 shows the cyclic voltammogram of the random-oriented $LiCoO_2$ thin film deposited for 3 h. As shown in Fig. 3, a large peak and two small peaks were observed. The peak separation of the redox couple was again about 40 mV, indicating that the electronic conductivity is high enough for electrochemical measurements. The cyclic voltammograms in Figs. 3 and 4 are very similar except for the current intensities. This difference in current intensity is principally due to the difference in insertion/extraction sites for Li-ion. The details will be discussed later.

3.3.3. AC impedance spectroscopy

AC impedance measurements were carried out using a three-electrode cell. As shown in Fig. 5, Nyquist plots gave one semi-circle and a linear line for the *c*-axis-oriented $LiCoO_2$

thin film electrode at potentials between 3.92 and 4.40 V. Since the electric conductivity of $LiCoO_2$ was sufficiently high as described above, the semi-circle can be ascribed to charge (Li-ion) transfer resistance at the $LiCoO_2$ / electrolyte interface at the given potentials. Below 3.8 V, only blocking-electrode-type behavior was observed. As is clear from the cyclic voltammograms in Figs. 3 and 4, little current is observed at potentials below 3.8 V. Therefore, this blocking-electrode-type behavior is quite valid.

To confirm the assignment of the semi-circle in Fig. 5 as charge transfer resistance, impedance measurements were carried out with different concentrations of Li salt. Liquid electrolyte of 0.125 – 1.00 mol dm^{-3} $LiClO_4$ / PC was used and the potential was kept constant at 3.92 V. As shown in Fig. 6, the diameter of the semicircle increased as the salt concentration decreased. This indicates that these semi-circles are derived from the relaxation processes related to Li-ion. The correlation between the Li salt concentration and the reciprocal of the charge transfer resistance was plotted in Fig. 7, and a linear relationship was observed. Generally, exchange current i_0 is expressed as $i_0 = FAk^0C$ (F: Faraday constant, A: area, k^0: standard heterogeneous rate constant, C: concentration of species) [6]. On the other hand, the charge transfer resistance is described as $R_{ct} = RT / nFi_0$ (R: gas constant, T: absolute temperature, n: stoichiometric number of electrons involved in an electrode reaction) [6]. These equations can be rewritten as $i_0 = (RT/ nF)\times 1/R_{ct}$. Based on these equations, we obtain $i_0 = FAk^0C = (RT/ nF)\times 1/R_{ct}$. Therefore, the reciprocal of charge transfer resistance is proportional to the Li salt concentration. From Fig. 7, the assignment in the Nyquist plot is considered to be reasonable.

The effects of orientation on charge transfer resistance are shown in Fig. 8 (a) and 8 (b). *C*-axis-oriented and random-oriented films were used for Figs. 8 (a) and 8 (b), respectively. As shown in Fig. 8 (a), charge transfer resistance appeared at around 3.9 V and then decreased drastically. Charge transfer resistance then remained constant up to 4.2 V and increased gradually. As Shown in Fig. 8 (b), the behavior of the charge transfer resistance of the random-oriented film is almost similar to that of *c*-axis-oriented film, but the charge transfer resistance increased at a lower potential of 4.1 V. In addition to this difference in the onset potential when the charge transfer resistance increased, the values of the charge transfer resistance were also quite different. The minimum charge transfer resistance for

c-axis-oriented film was 10-fold greater than that for random-oriented film. This large difference in charge transfer resistance was due to the orientation of $LiCoO_2$ thin films. In the present system, the resistance is affected by the number of active sites that Li-ions can intercalate and de-intercalate at the $LiCoO_2$ thin film. Since the area of the working electrode is restricted by the o-ring, Li-ion can intercalate and de-intercalate only at defects on the film surface for c-axis-oriented film. On the other hand, random-oriented film has many active sites for Li-ion to intercalate/de-intercalate. Consequently, the charge transfer resistance of c-axis-oriented film was greater than that of random-oriented film. The number of active sites seems to influence the onset potential at which the charge transfer resistance increased. Once the charge transfer resistance increased at potentials above 4.2 V, the resistance did not decrease with a decrease in the electrode potential, indicating that an irreversible reaction such as electrolyte oxidation (decomposition) occurs at higher potentials [7]. This electrolyte decomposition should occur at active sites of $LiCoO_2$ thin film, and therefore electrolyte oxidation occurs more readily at more negative potentials when the random-oriented film is used.

Figure 9 shows the temperature-dependence of the charge transfer resistance of c-axis-oriented $LiCoO_2$ thin film (squares) and random-oriented $LiCoO_2$ thin film (circles). By the least-squares method, the apparent activation energies for Li-ion transfer were determined to be 46±7.3 $kJmol^{-1}$ for *c*-axis-oriented thin film and 48±6.1 $kJmol^{-1}$ for random-oriented thin film at 4.10 V. The activation energies appeared to be almost the same regardless of the orientation of $LiCoO_2$. This result indicates that a high activation barrier exists at the $LiCoO_2$ / electrolyte interface and the activation energy is not influenced by the orientation of the electrode materials. Our recent studies on large activation barriers at the electrode / electrolyte interface revealed that de-solvation is responsible for the activation energy [8-10]. Therefore, the present results seem to be quite valid.

3.4. Conclusions

Li-ion transfer at the interface between an electrolyte and $LiCoO_2$ thin films with different orientations was studied. The orientation of the $LiCoO_2$ thin film electrode strongly affects the charge transfer resistance, but does not affect the activation energy for charge transfer. These results indicate that the orientation may play an important role in decreasing the internal resistance in lithium ion batteries.

References

[1] B, Neudecker, N.J. Dudney B.J. Bates, *J.Electrochem. Soc.*, **147** (2000) 517
[2] B.J. Bates, N.J. Dudney, B, Neudecker, A. Ueda and C.D. Evans, *Solid State Ionics*, **135** (2000) 33.
[3] M. Inaba, Y. Iriyama, Z. Ogumi, Y. Todzuka and A. Tasaka, *J. Raman Spectroscopy*, **28** (1997) 613
[4] Y. Iriyama, M. Inaba, T. Abe and Z. Ogumi, *J. Power Sources*, **94** (2001) 175
[5] J.N. Reimers and D.R. Dahn, *J. Electrochem. Soc.*, **139** (1992) 2091
[6] A.J. Bard and L.R. Faulkner: Electrochemical Methodes, Fundamental and Applications, 2nd ed. (John Wiley & Sons,Inc, New York, 2000)
[7] D. Aurbach, *J. Power Sources*, **89** (2000) 206
[8] T. Abe, H. Fukuda, Y. Iriyama and Z. Ogumi, *J. Electrochem. Soc.*, **151** (2004) A1120
[9] F. Sagane, T. Abe, Y.Iriyama and Z. Ogumi, *J. Power Sources.*, **146** (2005) 749
[10] T. Doi, K. Miyatake, Y.Iriyama, T.Abe, Z. Ogumi and T. Nishizawa, *Carbon*, **42** (2004) 3183

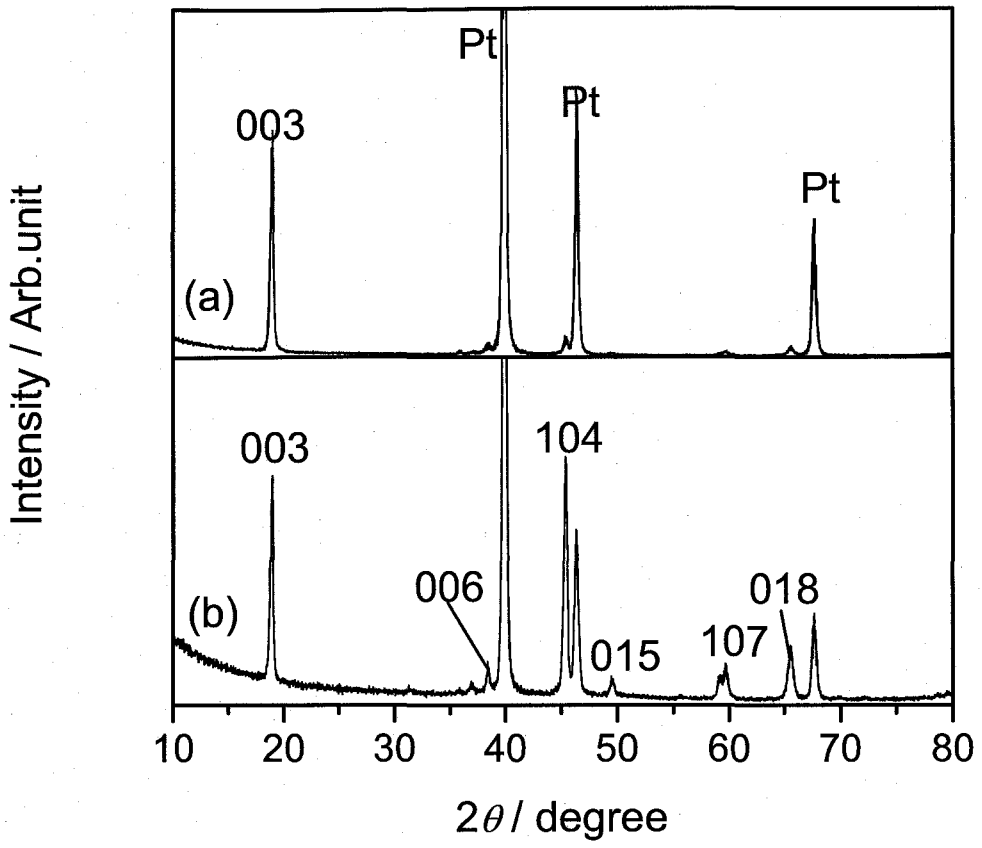

Fig 3.1. X-ray diffraction patterns of $LiCoO_2$ thin films deposited on Pt for (a) 1 h and (b) 3 h.

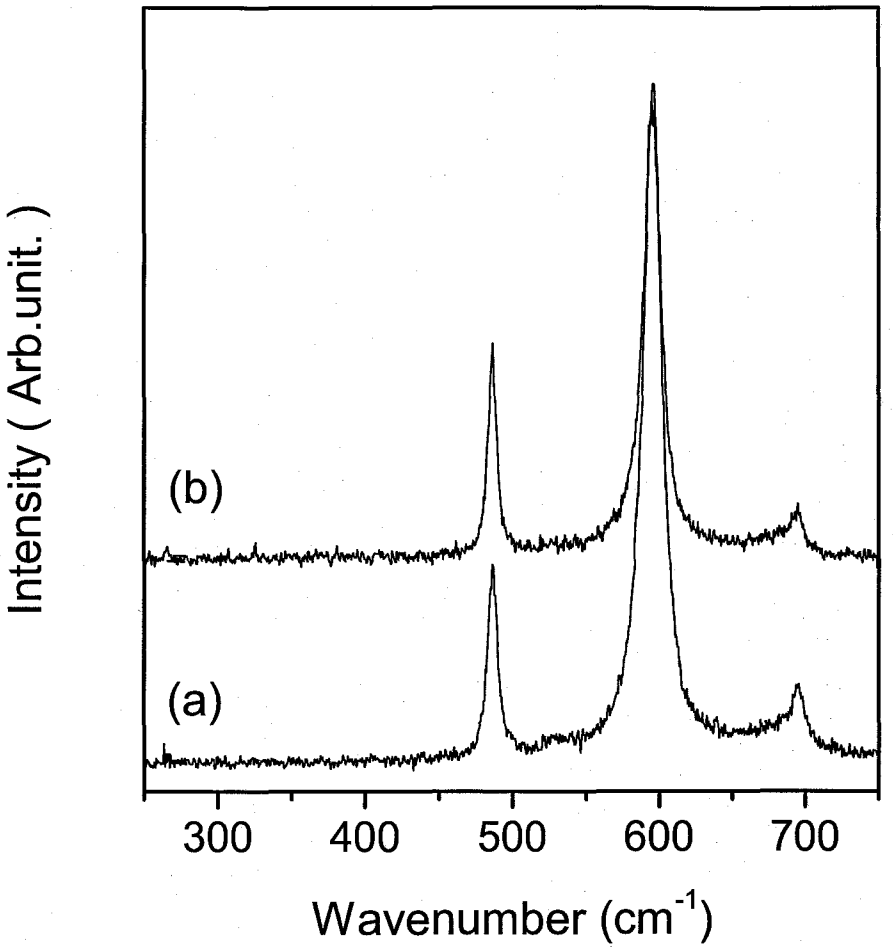

Fig 3.2. Raman spectra of $LiCoO_2$ thin films deposited on Pt for (a) 1 h and (b) 3 h.

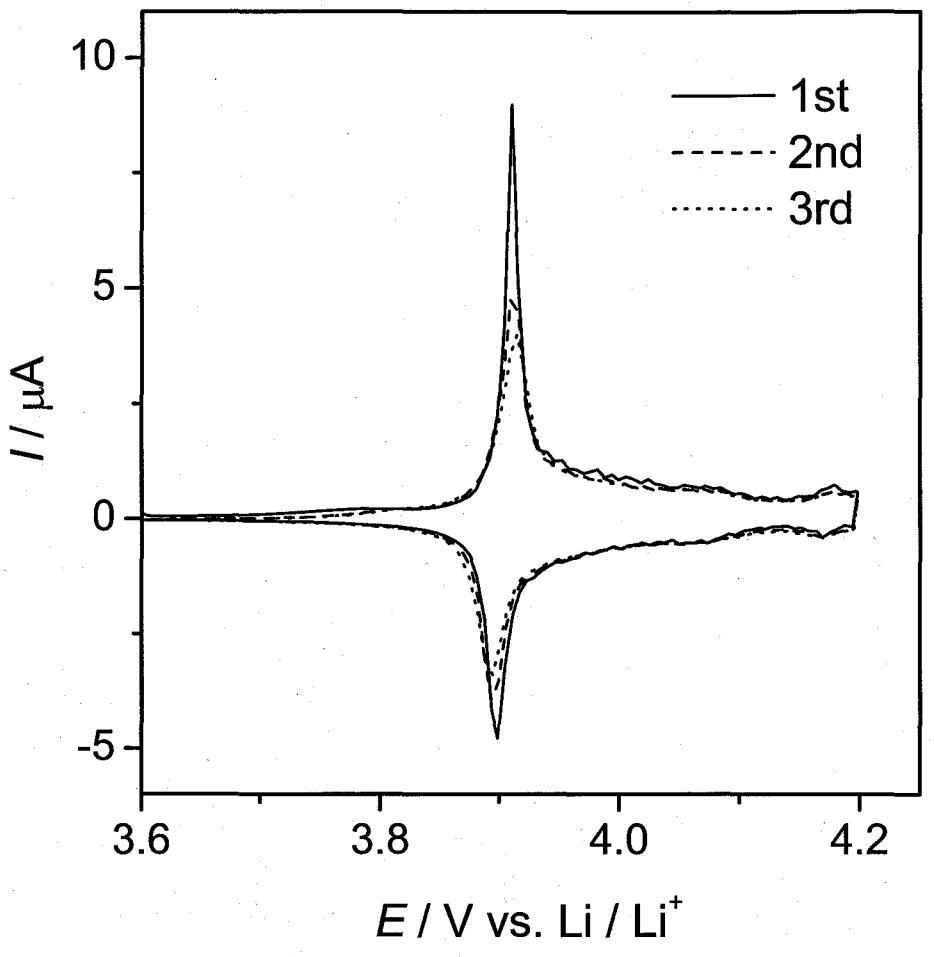

Fig 3.3. Cyclic voltammogram of $LiCoO_2$ thin film electrode deposited for 1 h in 1 mol dm^{-3} $LiClO_4$ / PC. Scanning rate = 0.1 mV / s.

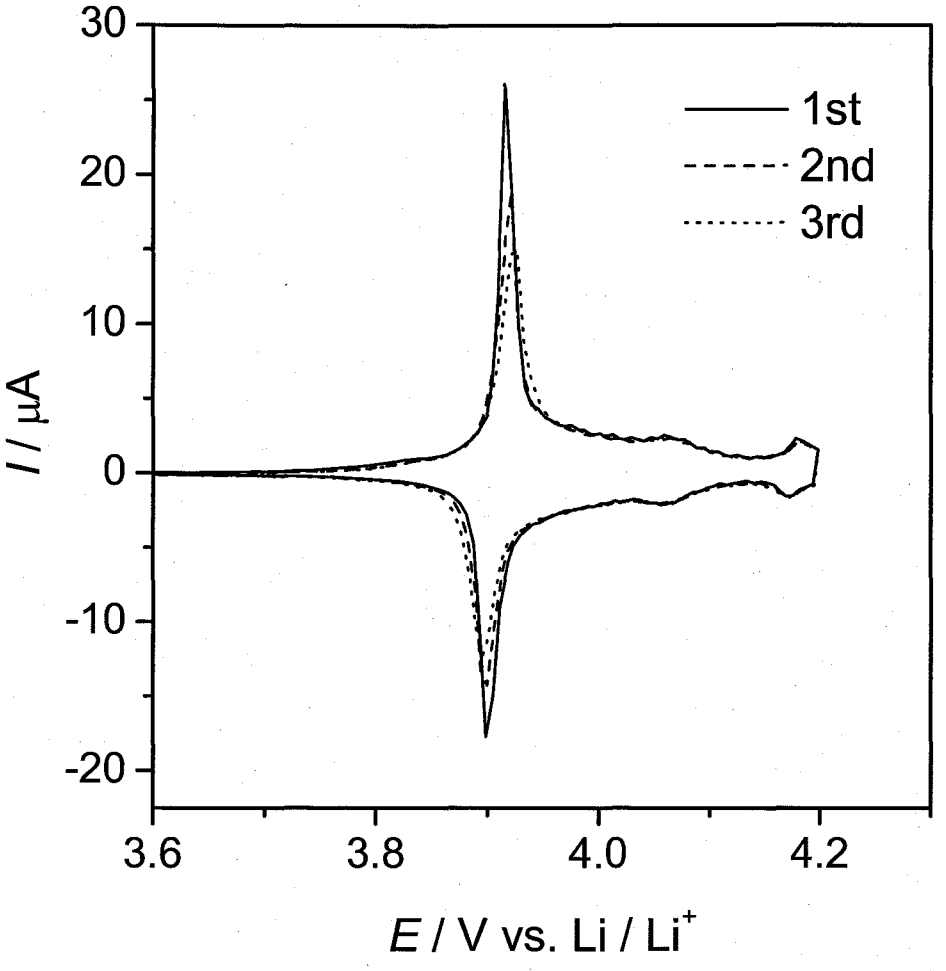

Fig 3.4. Cyclic voltammogram of $LiCoO_2$ thin film electrode deposited for 1 h in 1 mol dm^{-3} $LiClO_4$ / PC. Scanning rate = 0.1 mV / s.

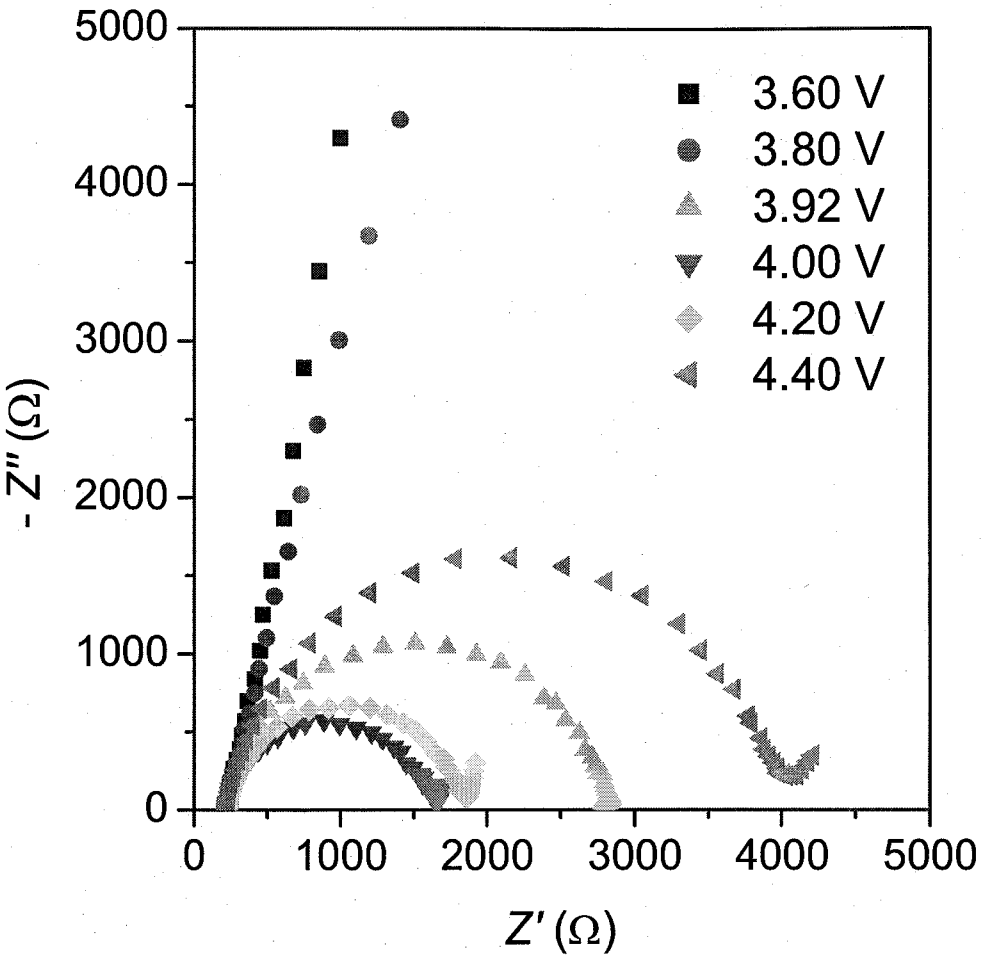

Fig 3.5. Nyquist plots of $LiCoO_2$ thin film deposited for 1 h in 1 mol dm^{-3} $LiCF_3SO_3$ / PC at potentials of 3.60, 3.80, 3.92, 4.00, 4.20, and 4.40 V.

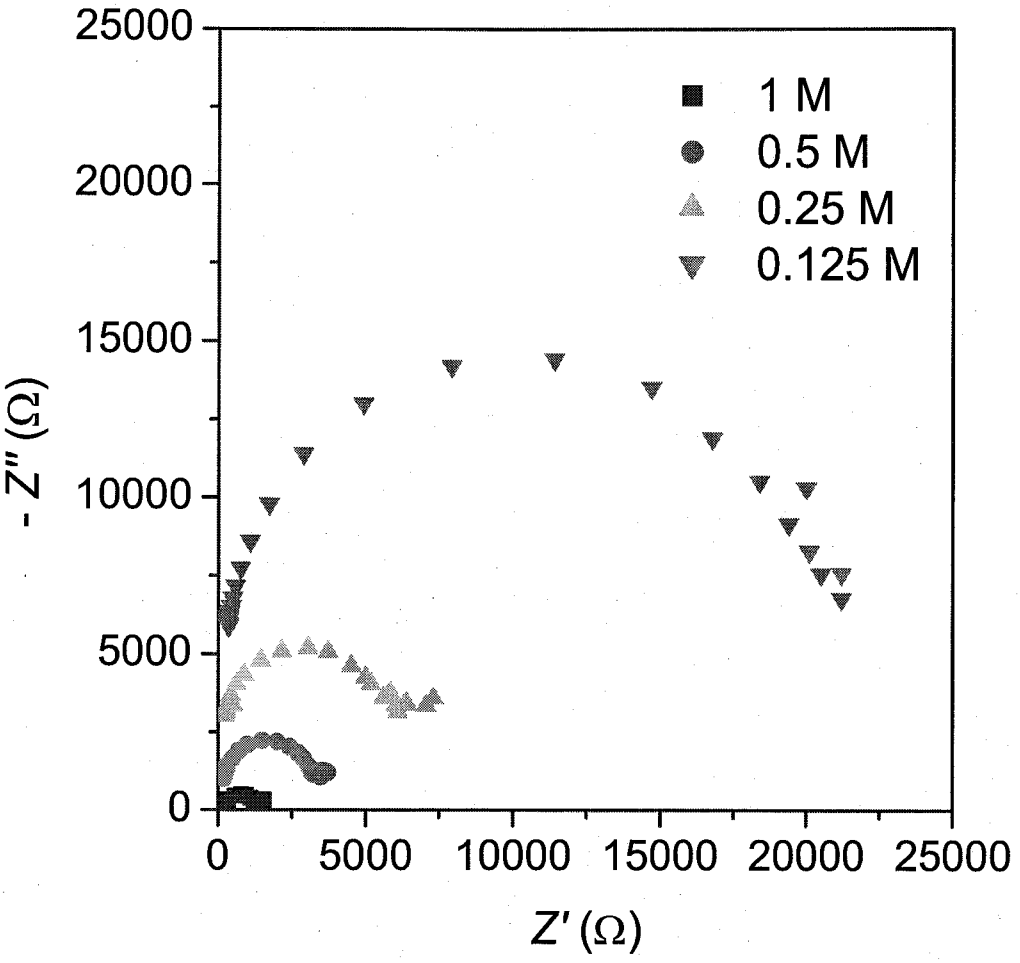

Fig 3.6. Nyquist plots of $LiCoO_2$ thin film deposited for 1 h in 1.0, 0.5, 0.25 and 0.125 mol dm^{-3} $LiCF_3SO_3$ / PC.

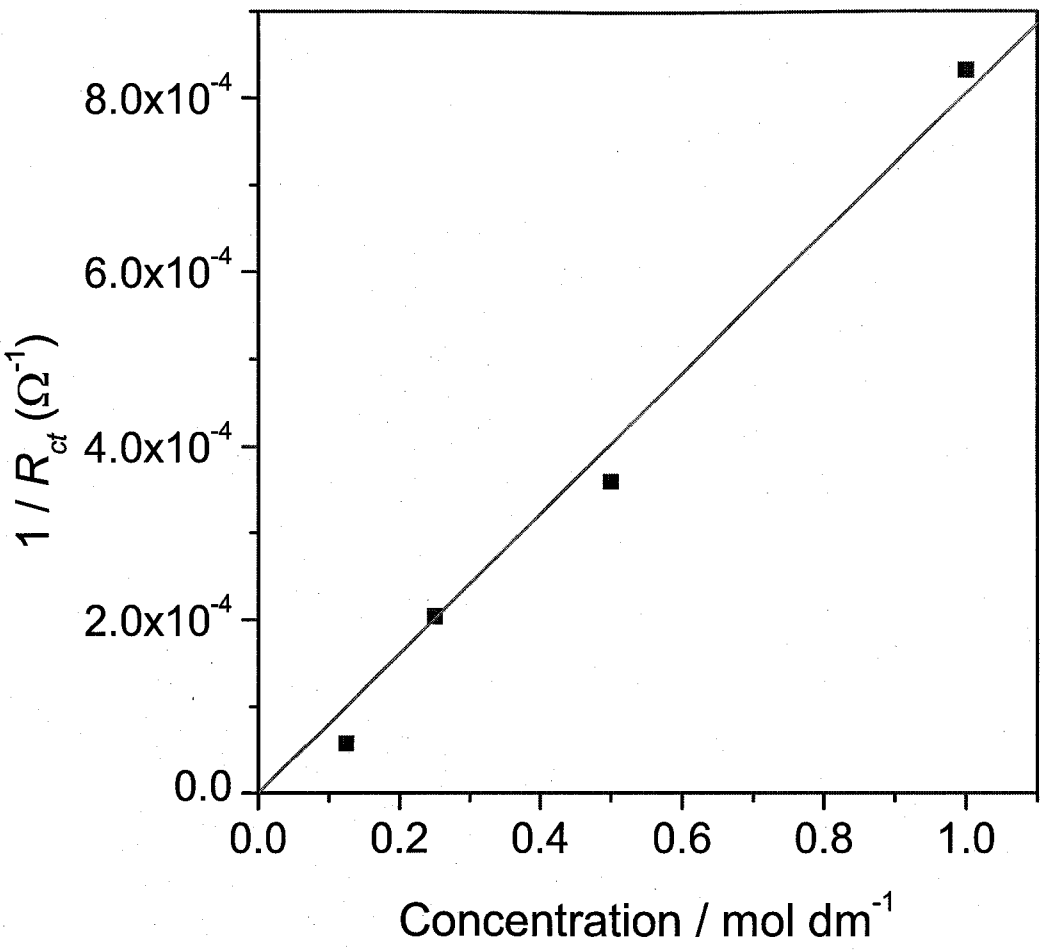

Fig.3.7. Concentration-dependence of the reciprocal of charge transfer resistance.

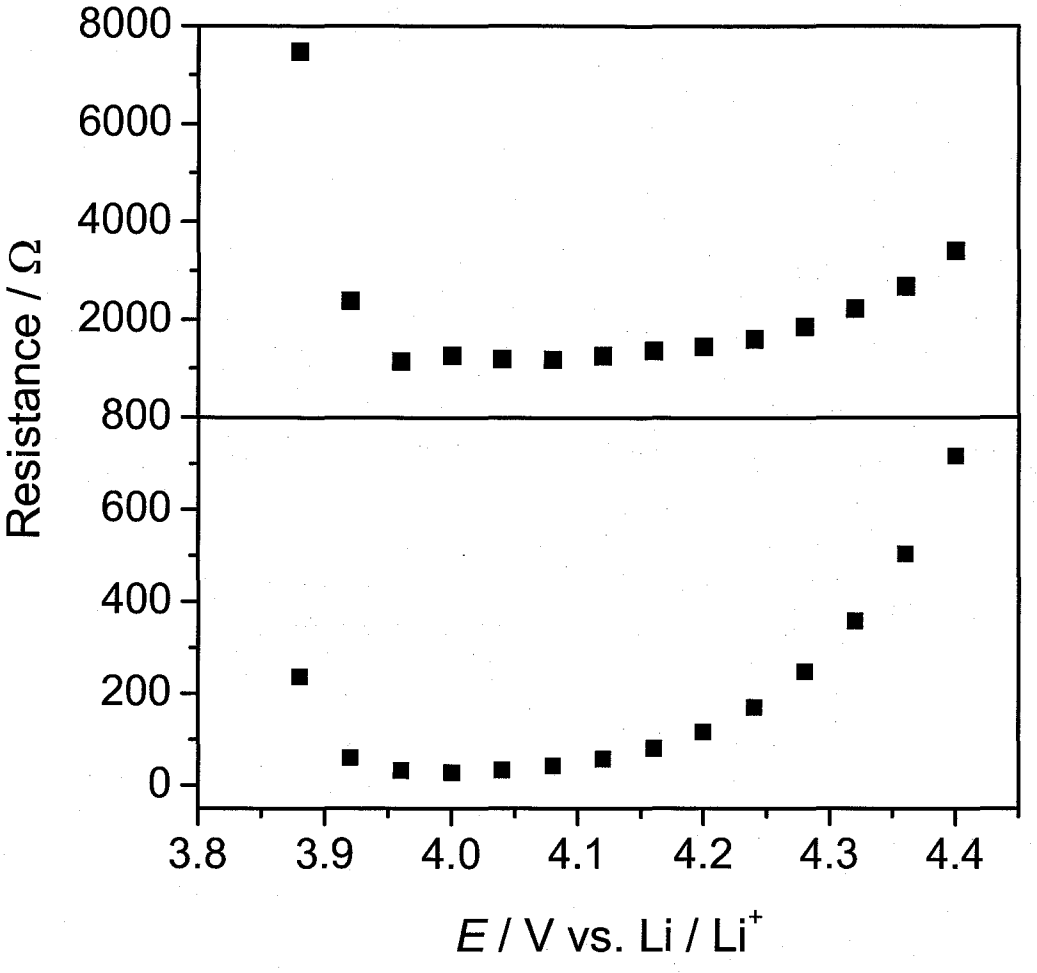

Fig.3.8. Variation of the charge transfer resistance of an electrolyte / $LiCoO_2$ thin film [deposited for (a) 1 h and (b) 3 h] interface with the electrode potential.

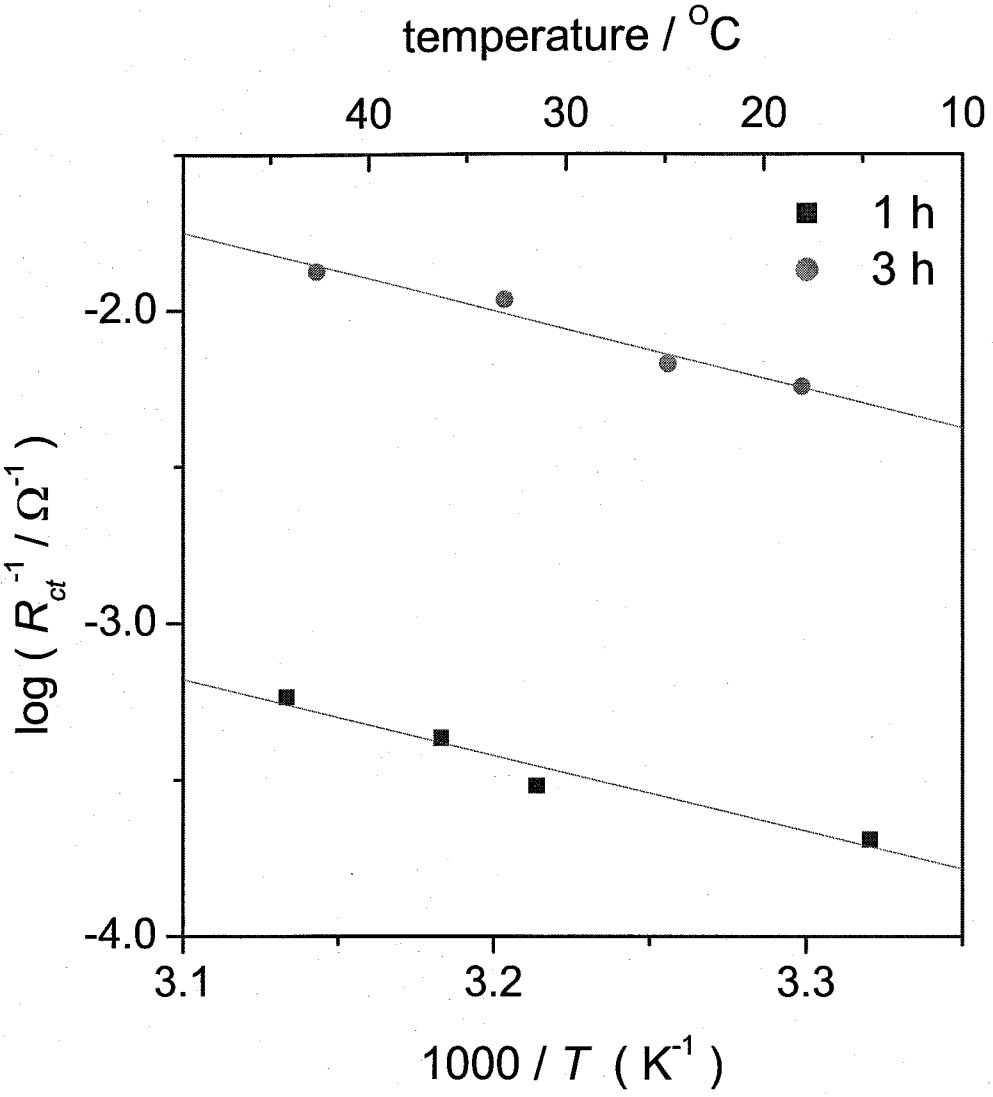

Fig 3.9. Temperature-dependence of the charge transfer resistance of an electrolyte / $LiCoO_2$ thin film [deposited for (a) 1 h and (b) 3 h] interface. Line is drawn by a least-squares method.

PART II

Effect of Electrolytes on Interfacial Lithium Ion Transfer

CHAPTER 4

Lithium ion transfer between Li_xCoO_2 and polymer gel electrolyte

4.1. Introduction

Lithium-ion batteries have been widely used in the field of portable electronic devices. Recently, due to limitations regarding the use of Cd, the application of lithium-ion batteries has been expanded to electric power tools, and Ni-Cd batteries are gradually being replaced by lithium-ion batteries. Two major driving forces underlie recent R&D on Li-ion batteries. One is the need to improve small-scale Li-ion batteries for use in electronic devices and the other is the need to enhance the performance of large-scale lithium-ion batteries for use in hybrid electric vehicles (HEV).

Several factors must be considered for the practical use of lithium-ion batteries in HEV. Among them, the enhancement of rate-performance and the improvement of safety are critical issues. We have focused on lithium-ion transfer at the electrode/electrolyte interface and found that there are large activation barriers for the transfer of lithium-ion at the interface [1-10]. Based on our results thus far, we have proposed a design for lithium-ion batteries with high rate-performance. Although enhancement of the

rate-performance of lithium-ion batteries needs to be investigated further, in this study we focused on the serious issue of safety.

Solid polymer electrolytes have been extensively studied since Wright et al. [11] reported an acceptable ion-conductive complex of alkali metal salts and poly(ethylene oxide). Solid polymer electrolytes have received considerable attention as promising materials for lithium-ion batteries due to advantages in safety, high energy density and ease of manufacture. However, some problems, such as low ionic conductivity and poor contact with active materials, still remain to be solved for the practical use of solid polymer electrolytes in lithium batteries. Poor contact between a polymer electrolyte and the active electrode material is a very serious problem, and hence polymer gel electrolytes, which consist of polymer matrices, plasticizers, and lithium salt, have recently attracted attention probably because plasticizers in the polymer matrix enhance the compatibility between the electrolyte and the active electrode material. Polymer gel electrolytes enhance the safety of lithium-ion batteries compared with conventional liquid electrolytes.

Much work has been done on the optimization of the components of polymer gel electrolytes. However, little attention has been paid to interfacial reactions between electrodes and polymer gel electrolytes, despite the fact that the battery reaction rate depends on the rate of interfacial reactions and the diffusion rate through active matrices.

We report here lithium-ion transfer at the interface between $LixCoO_2$ and PVdF-based polymer gel electrolytes using AC impedance spectroscopy.

4.2. Experimental

4.2.1. Preparation of polymer gel electrolytes

Polymer gel electrolytes were prepared from polyvinylidene fluoride (PVdF), polyethyleneglycol dimethyl ether (PEGDME) and lithium salts such as $LiCF_3SO_3$, $LiN(CF_3SO_2)(C_4F_9SO_2)$, and others. PEGDMEs with molecular weights of 250, 500 and 1000 were used. The weight ratio of PVdF to PEGDME was set at 3 : 7. $LiCF_3SO_3$ was

added at a ratio of EO (ethylene oxide unit) in PEGDME / Li = 25. A mixture of PVdF, PEGDME, and $LiCF_3SO_3$ was melted at 407 K, and the solution was then cooled in a Teflon template to form transparent gel electrolytes 300-mm thick. The ionic conductivities of the polymer gel electrolytes were determined by AC impedance spectroscopy with a Sorlatron 1255.

4.2.2. Preparation of $LiCoO_2$ composite electrode

A $LiCoO_2$ composite electrode was prepared from $LiCoO_2$, acetylene black, and polymer gel electrolytes, with weight ratios of 20 wt%, 7 wt%, and 73 wt%, respectively. These weight ratios gave sufficient electric and ionic conductivities for the resulting electrode.

4.2.3. Preparation of $LiCoO_2$ thin film electrode

$LiCoO_2$ thin films were prepared by pulsed laser ablation using a KrF excimer laser with a wavelength of 248 nm (Japan Storage Battery, EXL-210). The substrate was a polished Pt plate. The detailed conditions for preparation were reported previously [12]. The resulting $LiCoO_2$ thin films were characterized by X-ray diffraction to be highly oriented along the *c*-axis.

4.2.4. AC impedance measurement

Lithium-ion transfer at the interface between $LixCoO_2$ and polymer gel electrolytes was studied by AC impedance spectroscopy using a Sorlatron 1255 in the frequency range of 100 kHz – 1 mHz. A three-electrode cell was used regardless of the electrodes. Li metal was used for the counter and reference electrodes. Measurement took place from 3.40 V to 4.15 V. Each potential was held for 5 h to reach a steady state.

4.3. Results and Discussion

Figure 1 shows the ionic conductivities of PVdF-based polymer gel electrolytes with various plasticizers plotted against reciprocal temperatures. With an increase in the molecular weight of the plasticizers, the temperature-dependence of ionic conductivity became VTF-type. Polymer gel electrolytes using PEGDME250 gave ionic conductivities higher than $10^{-3.5}$ S/cm at room temperature, while other polymer gel electrolytes gave somewhat lower conductivities due to the high viscosities of the plasticizers. For polymer gel electrolytes with PEGDME1000, a rapid increase in conductivity can be seen at around 303 K. At these temperatures, PEGDME1000 melts, resulting in an increase in conductivity.

Figure 2 shows Nyquist plots for a Li / polymer gel electrolyte / $LiCoO_2$ composite electrode cell at various electrode potentials. Open squares, circles, triangles, and solid circles denote the potentials 3.464, 3.840, 3.920, and 4.000 V, respectively. The inset figure shows a Nyquist plot for an electrode containing only PVdF and acetylene black in 1 mol dm^{-3} $LiClO_4$/ethylene carbonate (EC) - diethyl carbonate (DEC) (1 : 1 by volume). The plasticizer is PEGDME250 and the lithium salt is $LiCF_3SO_3$. At a potential of 3.464 V, only one semi-circle was observed in the high frequency region, and in the middle to lower frequency region, the electrode exhibited typical blocking-electrode-type behavior. In contrast, two semicircles were observed at potentials above 3.84 V, as shown in Fig. 2. In the high frequency region, resistance was independent of the potential, while in the middle to lower frequency region resistance depended on the potential. The characteristic frequencies of the latter semi-circles were around 1 Hz. To characterize these Nyquist plots, we first fabricated a composite electrode without $LiCoO_2$. The Nyquist plot is shown in the inset in Fig. 2. In the absence of $LiCoO_2$ as an active material, a similar semi-circle was observed in the higher frequency region. Therefore, the semi-circle at the higher frequency region in Fig. 2 may not be due to the relaxation process related to $LiCoO_2$, but rather to the electric contact resistance of the electrode. Hence, it is very reasonable that the semi-circle at the lower frequency region remains unchanged.

We next used liquid electrolytes containing various concentrations of $LiClO_4$, and

studied reactions at the electrode/electrolyte interface. In this case, the composite $LiCoO_2$ electrode consists of $LiCoO_2$, PVdF, and acetylene black, at weight ratios of 85 wt%, 10 wt%, and 5 wt%, respectively. Figures 3(a), 3(b), and 3(c) show Nyquist plots for the interfacial reactions between a $LiCoO_2$ electrode and propylene carbonate (PC) solutions containing 0.125, 0.250, and 0.500 mol dm^{-3} $LiClO_4$, respectively. The potential was kept constant at 3.90 V. The onset values of Z' are superimposed to make it easier to compare the low frequency region. The first semi-circle observed in the higher frequency region is almost unchanged, which indicates that these relaxation processes are independent of the cation or anion. This result is in good agreement with the above suggestion. In contrast, the dependency of the second semi-circles observed in the lower frequency region on the electrolyte concentration reveals that lithium-ion transfer at the interface between $LiCoO_2$ and the electrolyte is responsible for the observed semi-circle in AC impedance spectroscopy in Fig. 3.

Based on the above results, the semi-circle in the higher frequency region in Fig. 2 should be ascribed to contact resistance in the electrode, and that in the lower frequency region can be identified as charge (lithium-ion) transfer resistance.

When a thin film electrode of $LiCoO_2$ was used, the Nyquist plot became very simple. Nyquist plots for the liquid electrolyte / $LiCoO_2$ thin film interface are shown in Fig. 4. The electrolyte was 1 mol dm^{-3} $LiCF_3SO_3$ / PC. As is clearly shown in Fig. 4, only one semi-circle was observed at potentials higher than 3.92 V. At lower potentials, blocking-electrode-type behavior was again observed. Thus, the semi-circle in Fig. 4 was ascribed to charge transfer resistance.

Based on the above results and discussion, it is clear that the semi-circle observed in the lower frequency region in Fig. 2 is due to lithium ion transfer across the interface. Figure 5 shows the variation in charge transfer resistance with the electrode potential. Two different salts of $LiCF_3SO_3$ and $Li(CF_3SO_2)(C_4F_9SO_2)$, corresponding to solid squares and open circles, respectively, were used. Regardless of the salt used, the charge transfer resistance decreased in the initial stage of charging up to about 3.9 V vs. Li / Li^+ and then increased from about 4.0 V. After charging up to above 4.1 V, charge transfer resistance did not decrease with a decrease in potential, indicating that a surface film may be formed by

decomposition of the electrolyte. The minimum resistance of ca. 10 Ω can be seen at around 3.9 - 4.0 V.

Figure 6 shows the variation in charge transfer resistance with the electrode potential in the case of a $LiCoO_2$ thin film electrode. The charge transfer resistance decreased with an increase in electrode potential up to around 4.1 V, and then gradually increased up to 4.3 V. In this case, the rapid increase in charge transfer resistance seen in Fig. 5 is not observed. The contact area between a $LiCoO_2$ thin film electrode and liquid electrolyte was regulated by an o-ring to be 0.785 cm^2. Therefore, decomposition of the electrolyte is kinetically suppressed by the small reactive site. A minimum resistance of ca. 30 . was also seen at around 4.0 V. In Fig. 6, we used $LiCoO_2$ thin film electrodes, while in Fig. 5 we used powder $LiCoO_2$. Nevertheless, the charge transfer resistances are almost identical in order. The powder $LiCoO_2$ should give a lower charge transfer resistance due to the large reaction sites for the insertion and extraction of lithium-ion. When we consider the roughness factors, the minimum charge transfer resistance in Fig. 5 should be much smaller than those observed for a $LiCoO_2$ thin film electrode.

The large charge transfer resistance is principally due to the low wettability between $LiCoO_2$ and the polymer gel electrolyte. The large charge transfer resistances are more explicit for $LiCoO_2$ thin film electrode/polymer gel electrolyte interface as shown in Fig. 7. By comparing the results in Figs. 6 and 7, the minimum values of the charge transfer resistances differ by 5 times. Since lithium-ion cannot jump as an electron does, atomic contact between $LiCoO_2$ and the polymer gel electrolyte is essential for the insertion and extraction of lithium-ion at the electrode. The low wettability decreases the reactive sites and increases the charge transfer resistance. Before polymer gel electrolytes are used in lithium-ion batteries for high-rate use, wettability must be further improved.

The temperature-dependence of charge transfer resistance was studied to elucidate the activation energies. Figure 8 shows the variation in the temperature-dependence of charge transfer resistance for a Li_xCoO_2 / gel electrolyte cell at 3.8 V. The Li salt was $LiCF_3SO_3$ and the plasticizers were PEGDME250, 500, and 1000. Based on the slopes, the values of the activation energy were calculated to be 56.4, 60.6, and 71.4 kJ mol^{-1} for PEGDME250, 500, and 1000, respectively. The activation energy increases with an

increase in the molecular weight of the plasticizer. An increase in molecular weight has been reported to stabilize lithium-ion [13], leading to higher activation energies. Therefore, the plasticizer also plays an important role on lithium-ion kinetics at electrode. Higher molecular weight of plasticizer will give higher safety of lithium-ion batteries, but the lithium-ion kinetics will become slower.

3.4. Conclusions

Lithium-ion transfer at $LiCoO_2$ and polymer gel electrolyte interface was studied by AC impedance spectroscopy. The charge (lithium-ion) transfer resistances were found to be very large even for $LiCoO_2$ composite electrode due to the wettability between $LiCoO_2$ and polymer gel electrolyte. In addition, the plasticizer plays an important role on lithium-ion kinetics at $LiCoO_2$ electrode.

References

[1] T. Abe, F. Sagane, M. Ohtsuka, Y. Iriyama, Z. Ogumi, J. Electrochem.Soc., 152 (2005) A2151

[2] T. Doi, Y. Iriyama, T. Abe, Z. Ogumi, J. Electrochem. Soc., 152 (2005) A1521

[3] T. Doi, Y. Iriyama, T. Abe, Z. Ogumi, J. Power Sources., 142 (2005) 329

[4] T. Doi, K. Miyatake, Y. Iriyama, T. Abe, Z. Ogumi, Carbon, 42 (2004) 3183

[5] T. Abe, M. Ohtsuka, F. Sagane, Y. Iriyama, Zempachi Ogumi, J. Electrochem.Soc,.151 (2004) A1950

[6] T. Abe, H. Fukuda, Y. Iriyama, Z. Ogumi, J. Electrochem. Soc., 151 (2004) A1120

[7] I. Yamada, T. Abe, Y. Iriyama, Z. Ogumi, Electrochemi. Comm., 5 (2003) 502

[8] Y. Iriyama, H. Kurita, I. Yamada, T. Abe, Z. Ogumi, J. Power Sources., 137 (2004) 111

[9] T. Doi, Y. Iriyama, T. Abe, Z. Ogumi, Anal. Chem., 77 (2005) 1696

[10] F. Sagane, M. Ohtsuka, Y. Iriyama, T. Abe, Z. Ogumi, J. Power Sources., 146 (2005)

749

[11] D. E. Fenton, J. M. Parker and P. V. Wright, Polymer 14 (1973) 589.

[12] Y. Iriyama, M. Inaba, T. Abe, Z. Ogumi, J. Power Sources, 94 (2001) 175

[13] Johansson P, J. Phys. Chem. A .105 (2001) 9258

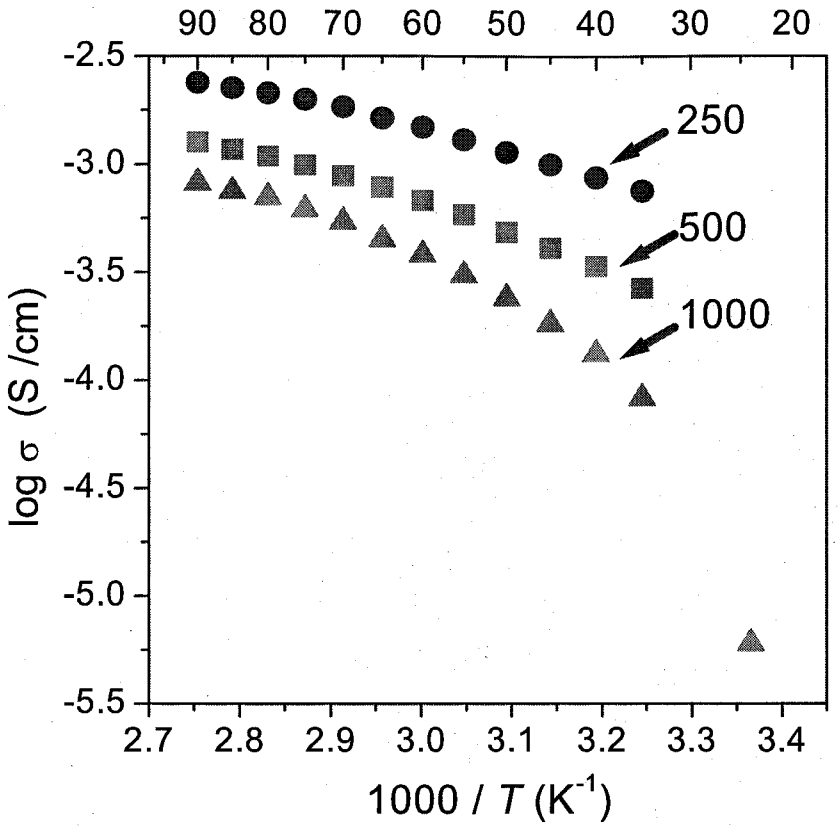

Fig 4.1. Temperature dependence of ionic conductivity for PVdF-based polymer gel electrolytes containing poly(ethyleneglycol)dimethylethers (M_w = 250, 500 and 1000). Numbers denote the molecular weight of poly(ethyleneglycol)dimethylethers.

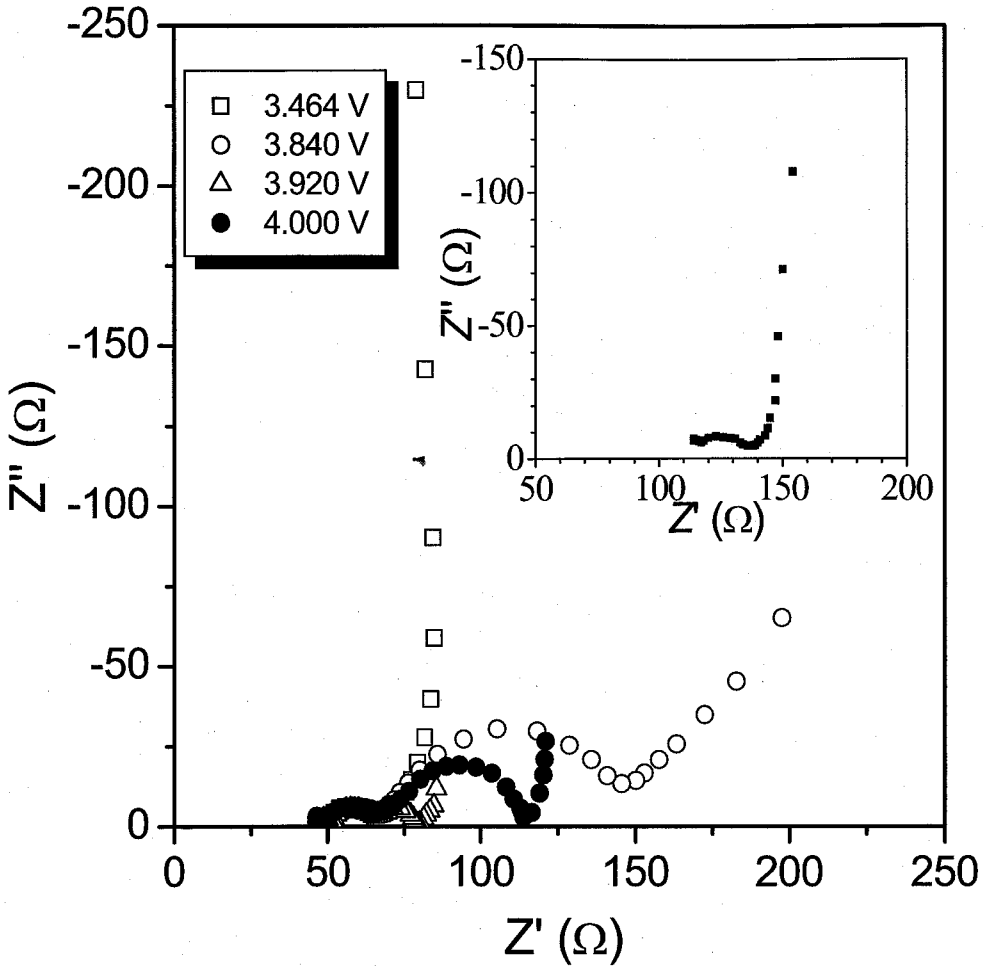

Fig 4.2. Nyquist plot for the cell of Li / polymer gel electrolyte / cathode composite at varioius electrode potentials. Open squares, circles, triangles, and solid circles denote the potentials of 3.464, 3.480, 3.920, and 4.000 V, respectively. Inset figure shows Nyquist plot for electrode containing only PVdF and acetylene black in 1 mol dm^{-3} $LiClO_4$ / EC-DEC (1:1) electrolyte.

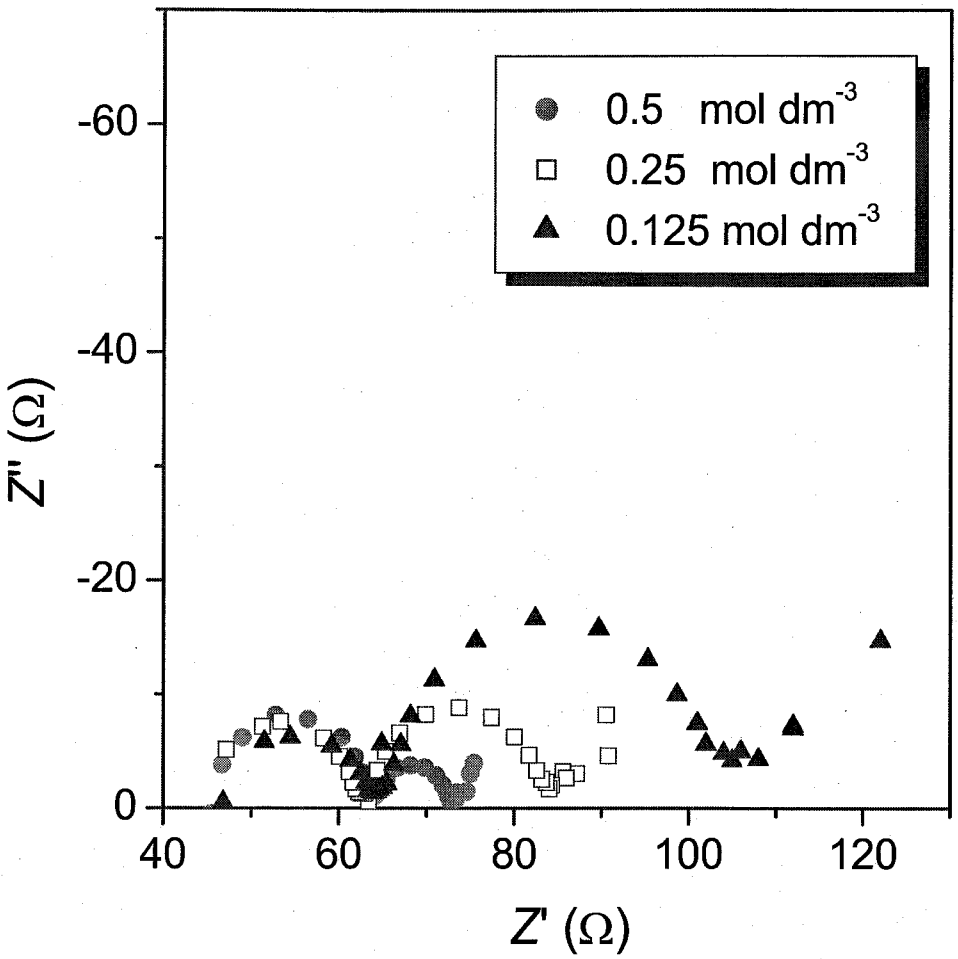

Fig 4.3. Nyquist plots for electrode consisting of $LiCoO_2$, PVdF, and acetylene black in PC electrolytes with various salt ($LiClO_4$) concentrations at electrode potential of 3.8 V (vs. Li/Li^+). Circles, squares, and triangles denote the concentrations of 0.500, 0.250, and 0.125 mol dm^{-3}, respectively. Bulk resistances of electrolytes are superimposed.

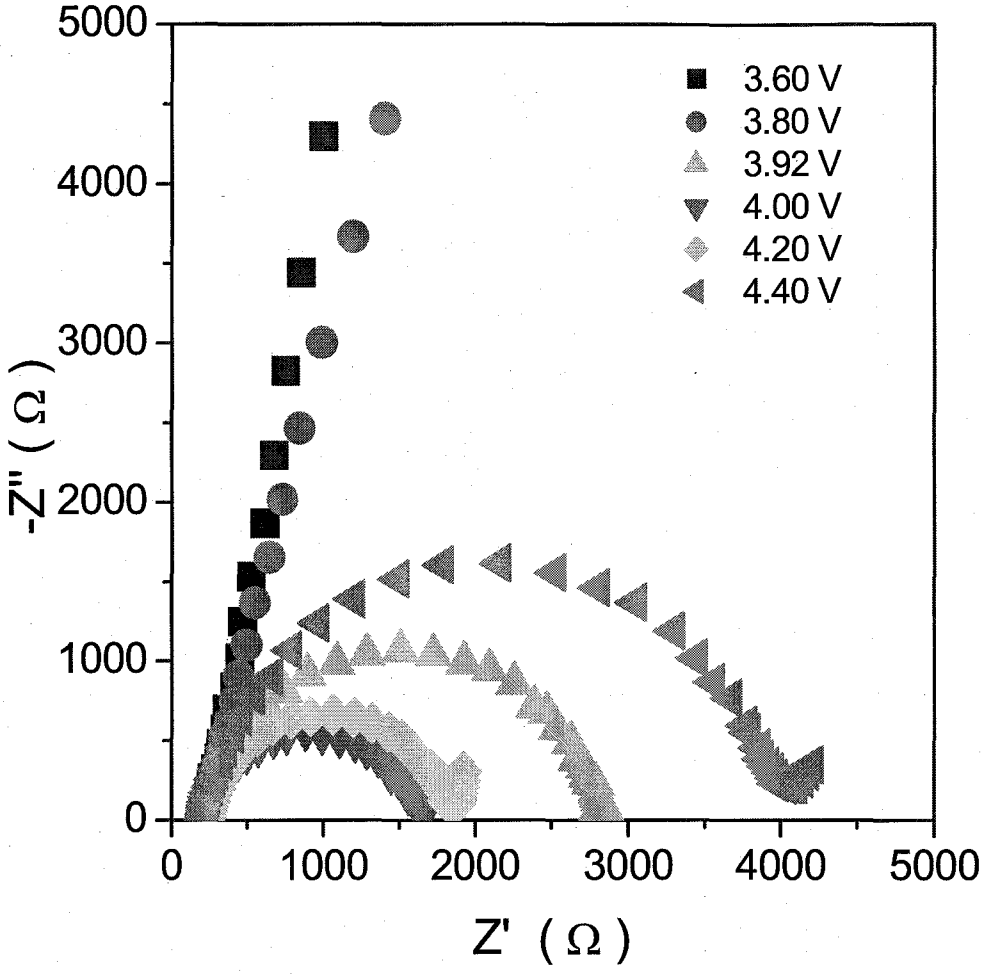

Fig 4.4. Nyquist plots for liquid electrolyte/$LiCoO_2$ thin film interface. Electrolyte is 1 M $LiCF_3SO_3$/PC.

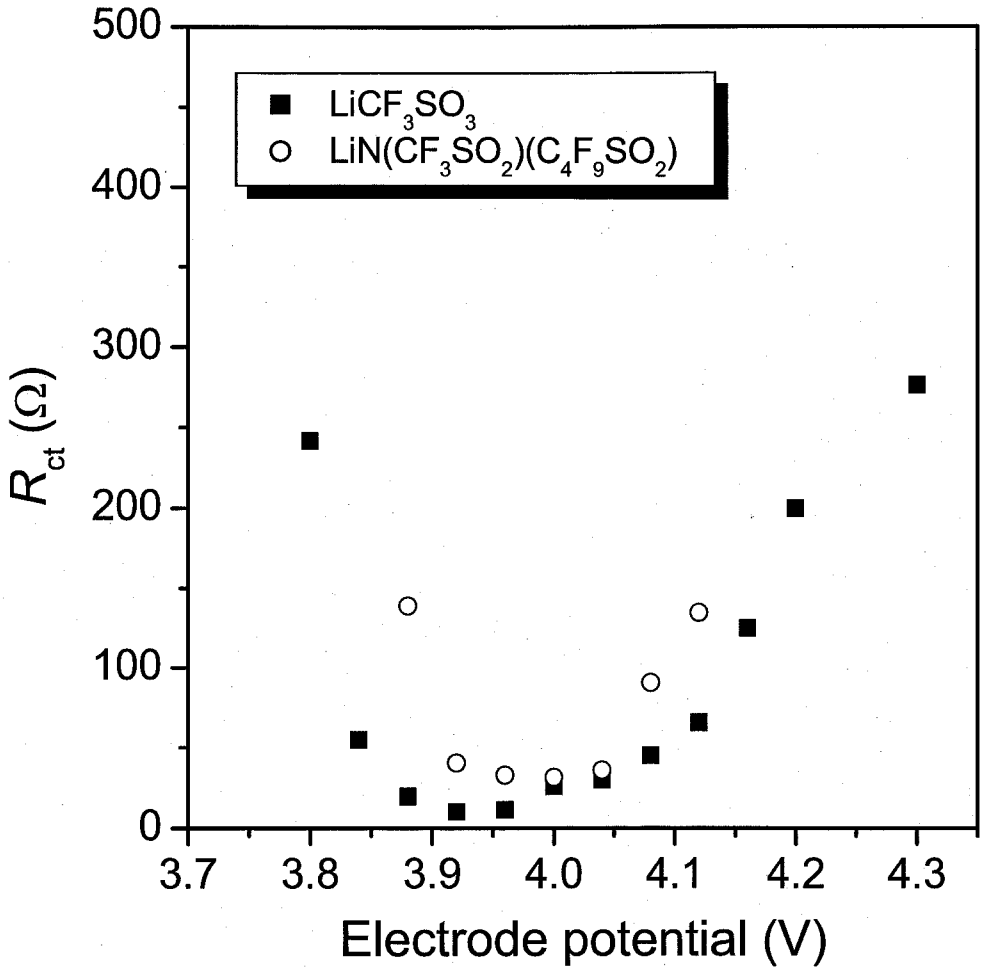

Fig 4.5. Variations of charge transfer resistances for Li_XCoO_2 /polymer gel electrolyte cell against electrode potentials. Plasticizer is PEGDME250. Li salt is (a) $LiCF_3SO_3$ and (b) $LiN(CF_3SO_2)(C_4F_9SO_2)$.

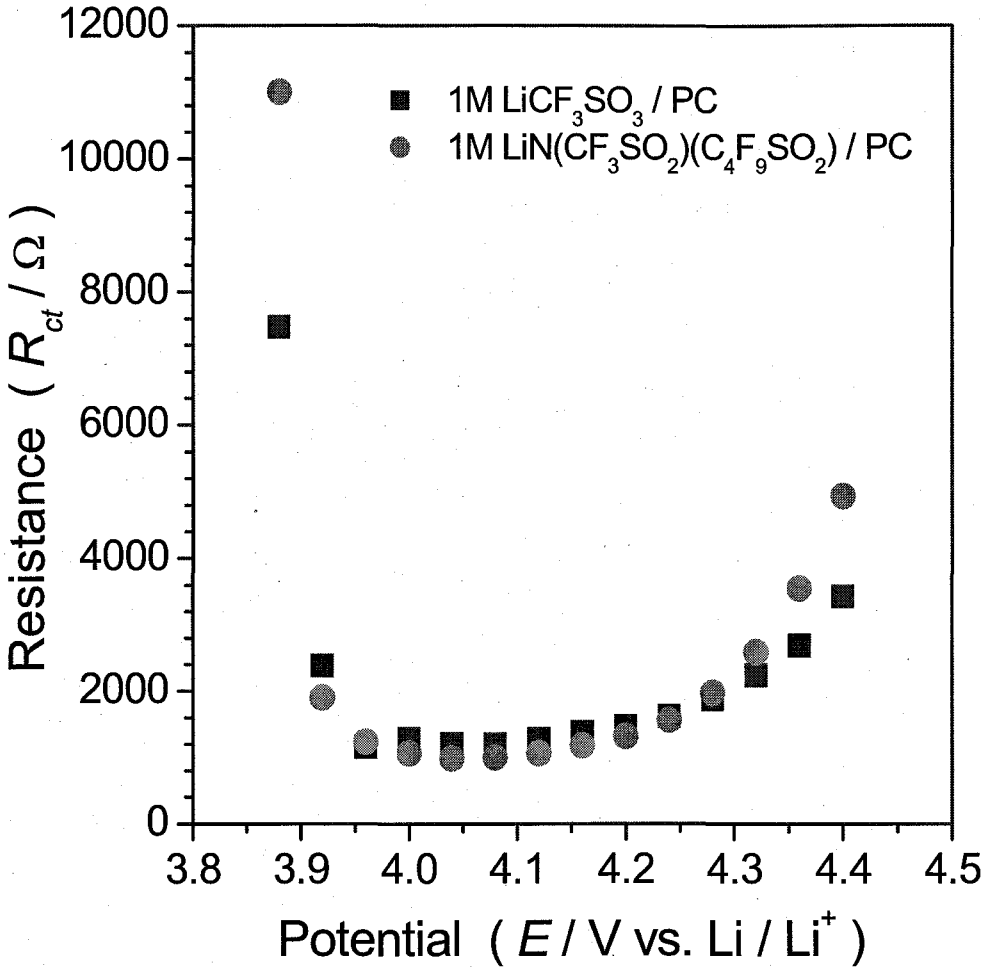

Fig 4.6. Variation of charge transfer resistance of liquid electrolyte/$LiCoO_2$ thin film interface against electrode potential.

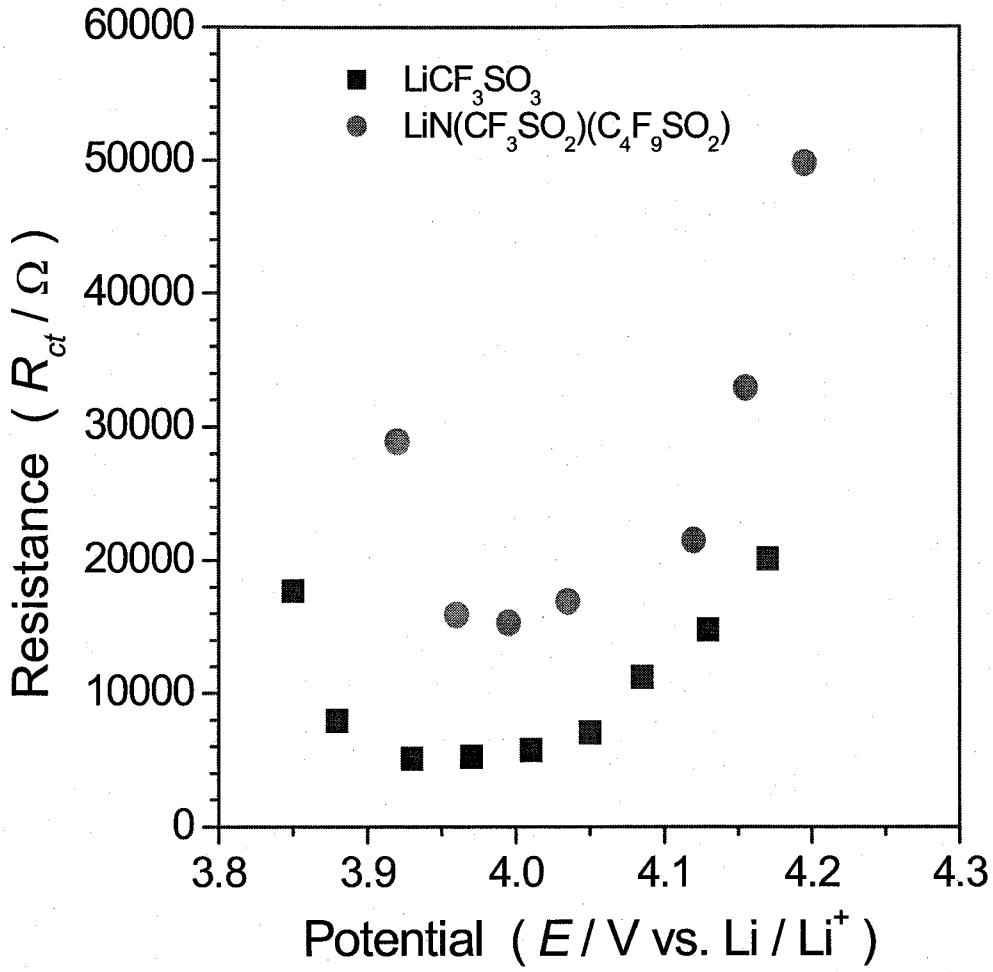

Fig 4.7. Variation of charge transfer resistance of polymer gel electrolyte / $LiCoO_2$ thin film interface against electrode potential.

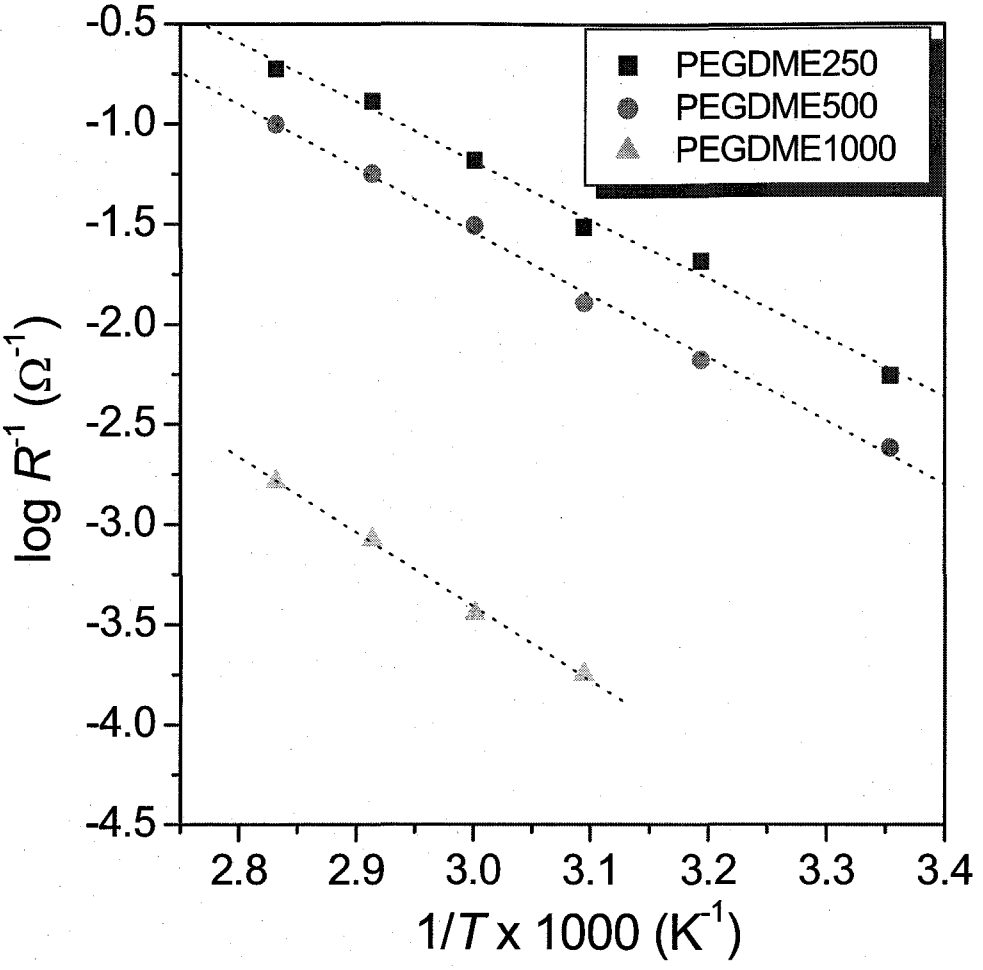

Fig 4.8. Temperature dependence of charge transfer resistances between polymer gel electrolytes and Li_XCoO_2 at electrode potential of 3.8 V. Squares, circles, and triangles denote PEGDME250, -500, and –1000, respectively.

CHAPTER 5

Lithium Ion Transfer at a Positive Electrode / Electrolyte Interface – Effect of Electrolyte -

5.1. Introduction

Li-ion secondary batteries have been used as power sources in portable electronic devices due to their high battery voltage and large gravimetric and volumetric energy densities. Recently, Li-ion batteries have also been expected to be useful as power sources in larger devices, such as power tools, electric vehicles (EV) and hybrid electric vehicles (HEV). These applications require Li-ion batteries with a high rate capability.

In Li-ion secondary batteries, charge and discharge reactions proceed by Li-ion transport between the positive and negative electrodes through an electrolyte. Therefore, high rate performance requires a high rate of Li-ion transport between the two electrodes. Li-ion transport in a single phase, such as diffusion through electrode materials and the electrolyte, has been well investigated [1-5]. However, Li-ion transfer at the interface between an electrode and the electrolyte is not yet well understood, even though such interfacial Li-ion transfer is an essential reaction in the battery system.

Interfacial Li-ion transfer is influenced by both the electrode and electrolyte. When the electrode is fixed, the effect of the electrolytes on Li-ion transfer can be studied systematically. The physical and chemical properties of electrolytes can be easily changed by the solvents and Li salts, and thus it should be interesting to study the effect of the solvents and Li salts used in electrolytes on interfacial Li-ion transfer.

For detailed studies, we prepared thin film electrodes by pulsed laser deposition to avoid the effects of binders and conductive additives. By using thin and very flat film electrodes, a structurally ordered interface can be fabricated to study on Li-ion transfer at the interface.

In this study, the effects of the electrolyte on Li-ion transfer at the electrode / electrolyte interface were examined by changing the electrochemical properties of the electrolyte.

5.2. Experimental

$LiCoO_2$ thin film was fabricated by pulsed laser deposition using a KrF eximer laser with a wavelength of 248 nm (Japan Storage Battery, EXL-210), with a polished Pt plate as a substrate at 873 K for 1 h. The details have been reported elsewhere [6]. The resulting $LiCoO_2$ thin films were characterized by X-ray diffraction to be highly oriented along the c-axis. The electrochemical properties of the thus-prepared $LiCoO_2$ thin film were studied by cyclic voltammetry using a three-electrode electrochemical cell (HSV-100, HOKUTO DENKO, Inc.). Li metal was used for the counter and reference electrodes. Unless noted otherwise, potentials were given by a Li metal potential.

Li-ion transfer at the electrolyte / $LiCoO_2$ thin film electrode interface was studied by AC impedance spectroscopy using a Radiometer, Voltalab 40 over a frequency range of 100 kHz to 10 mHz using the same three-electrochemical cell.

Electrolytes were prepared from lithium salts of $LiClO_4$, $LiCF_3SO_3$, $LiN(CF_3SO_2)(C_4F_9O_2)$ and solvents of propylene carbonate (PC), 1,2-dimethoxyethane (DME), 12-crown-4 ether. The concentration of electrolyte was adjusted to 1 mol dm^{-3}.

All experiments were conducted under an Ar atmosphere.

5.3. Results and discussion

Electrochemical properties of $LiCoO_2$ thin film were examined by cyclic voltammetry. Figure 1 shows a cyclic voltammogram of a $LiCoO_2$ thin film electrode prepared by pulsed laser deposition. A large peak at 3.92 V and very small peaks at 4.08 V and 4.12 V were observed in the cathodic direction, and can be attributed to the phase transition of $LiCoO_2$ [7]. Peak separation for the redox couple of 3.9 V was as small as 40 mV, suggesting that the ohmic drop was very small. Therefore, the electronic conductivity of the thin film electrode was considered to be sufficiently high for electrochemical measurements.

Li-ion transfer at the $LiCoO_2$ thin film / electrolyte interface was examined by AC impedance measurements. Figure 2 shows Nyquist plots of a $LiCoO_2$ thin film in 1 mol dm^{-3} $LiClO_4$ / PC at potentials of 3.80, 4.00, and 4.20 V. The Nyquist plot for 3.80 V was linear due to blocking-electrode-type behavior. On the other hand, a semi-circle and an almost vertical line were observed at 4.00 and 4.20 V. As is clear from Fig. 2, the semi-circle depends on the electrode potential. As mentioned above, the electrical conductivity of the thin film was sufficiently high, and therefore this semi-circle should be ascribed to Li-ion transfer resistance, i.e., charge transfer resistance. The vertical line indicates semi-infinite diffusion due to the thickness of the film (ca. 100 nm).

Figure 3 shows the effects of Li salts on the behavior of charge transfer resistance. Charge transfer resistance appeared at about 3.9 V, decreased drastically, and then remained fairly constant up to 4.2 V. Regardless of the Li salt used, the charge transfer resistance showed almost the same behavior. Thus, these anions of Li salt do not influence the behavior of charge transfer resistance.

Figure 4 shows the effects of the solvent on the behavior of charge transfer resistance. The solvents used included propylene carbonate (PC), 1,2-dimethoxyethane (DME), and a mixture of PC and 12-crown-4 ether. These solvents can be classified as esters and ethers. As clearly shown in Fig. 4, the behavior of charge transfer resistance varied according to the solvent used, indicating that the solvent affects interfacial Li-ion transfer. In particular, the onset electrode potential at which the charge transfer resistance

increased varied dramatically according to the solvent. Although the charge transfer resistance decreased up to 4.1 V regardless of the solvent, the charge transfer resistance increased at 4.1 V in DME, at 4.25 V in PC + 12-crown-4 ether, and at 4.3 V in PC. This increase in the charge transfer resistance is due to electrolyte decomposition at higher electrode potentials [8], resulting in a decrease in the number of reaction sites. Therefore, onset electrode potential at which charge transfer resistance increases is assumed to be an indicator of the tendency toward oxidative decomposition. Based on this assumption, the trend for oxidative decomposition was determined to be DME > 12-crown-4 ether > PC. It has been reported that ethers are oxidized at more negative electrode potentials than esters [9]. This agrees with the present results. The electronic structures of solvated Li-ion should also be considered for oxidative decomposition. Therefore, the solvation state of Li-ion is under further detailed investigation.

Figure 5 shows the temperature-dependence of the charge transfer resistance in PC and a mixture of PC and 12-crown-4 ether. By the least-squares method, the apparent activation energies for Li-ion transfer were determined to be 46 ± 7.3 $kJmol^{-1}$ for PC and 59 ± 4.7 $kJmol^{-1}$ for a mixture of PC and 12-crown-4 ether. The difference in activation energies is due to the presence of 12-crown-4 ether. Since the interaction between Li-ion and 12-crown-4 is stronger than that between Li-ion and PC based on a calculation using Gaussian 98, the 12-crown-4-based electrolyte gave a greater activation energy. Thus, the difference in activation energies reflects the solvation energy, indicating that the rate-determining step should be a de-solvation process.

5.4. Conclusions

The effect of the electrolyte on Li-ion transfer at a $LiCoO_2$ / electrolyte interface was studied by AC impedance measurements. Based on the dependency of charge transfer resistance on the electrode potential, the anions of Li salts used in the present work did not influence interfacial Li-ion transfer. In contrast, the solvent strongly affected Li-ion transfer. In particular, the onset electrode potential at which the charge transfer resistance increased

strongly depended on the solvent. Activation energies also depended on the solvent used and were correlated with the electron-donating ability of the solvent.

References

[1] A. Van der Ven and G. Ceder, Electrochem. Solid State Lett. 3 (2000) 301

[2] A. Funabiki, M. Inaba and Z. Ogumi, J. Power Sources 68 (1997) 227

[3] A. Noda, K. Hayamizu and M. Watanabe, J. Phys. Chem. B 105 (2001) 4603

[4] A. Funabiki, M. Inaba, Z. Ogumi, S. Yuasa, J. Otsuji and A. Tasaka, J. Electrochem. Soc. 145 (1998) 172

[5] Y. Iriyama, T. Abe, M. Inaba and Z. Ogumi, Solid State Ionics 135 (2000) 95

[6] Y. Iriyama, M. Inaba. T. Abe and Z. Ogumi, J. Power Sources 94 (2001), 175

[7] J.N. Reimers and D.R. Dahn, J. Electrochem. Soc. 139 (1992) 2091

[8] D. Aurbach, J. Power Sources 89 (2000) 206

[9] K. Nishimura, M. Mizumoto, H. Momose and T. Horiba, DENKI KAGAKU, 63 (1995) 802

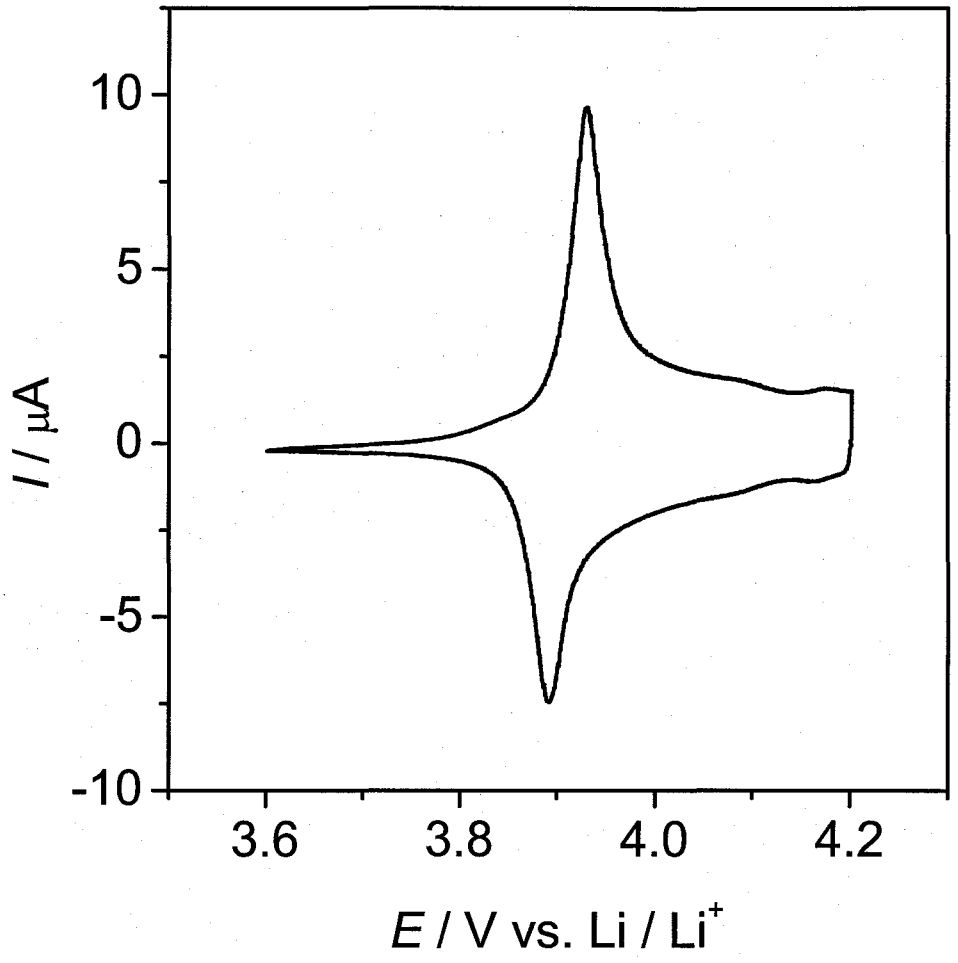

Fig 5.1 . Cyclic voltammogram of a $LiCoO_2$ thin film electrode. Scan rate is 0.1 mV / sec.

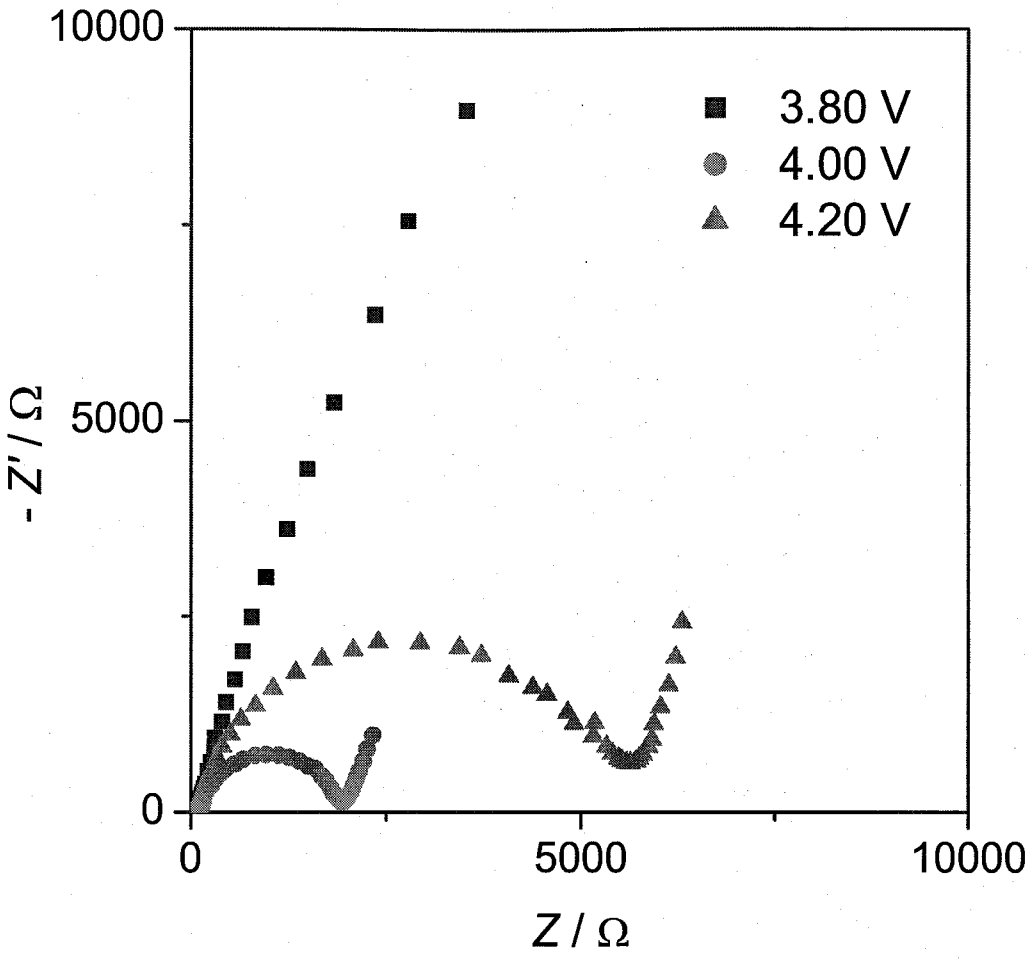

Fig 5.2 .Nyquist plots of $LiCoO_2$ thin film deposited for 1 h in 1 mol dm^{-3} $LiClO_4$ / PC at potentials of 3.80, 4.00, and 4.20 V.

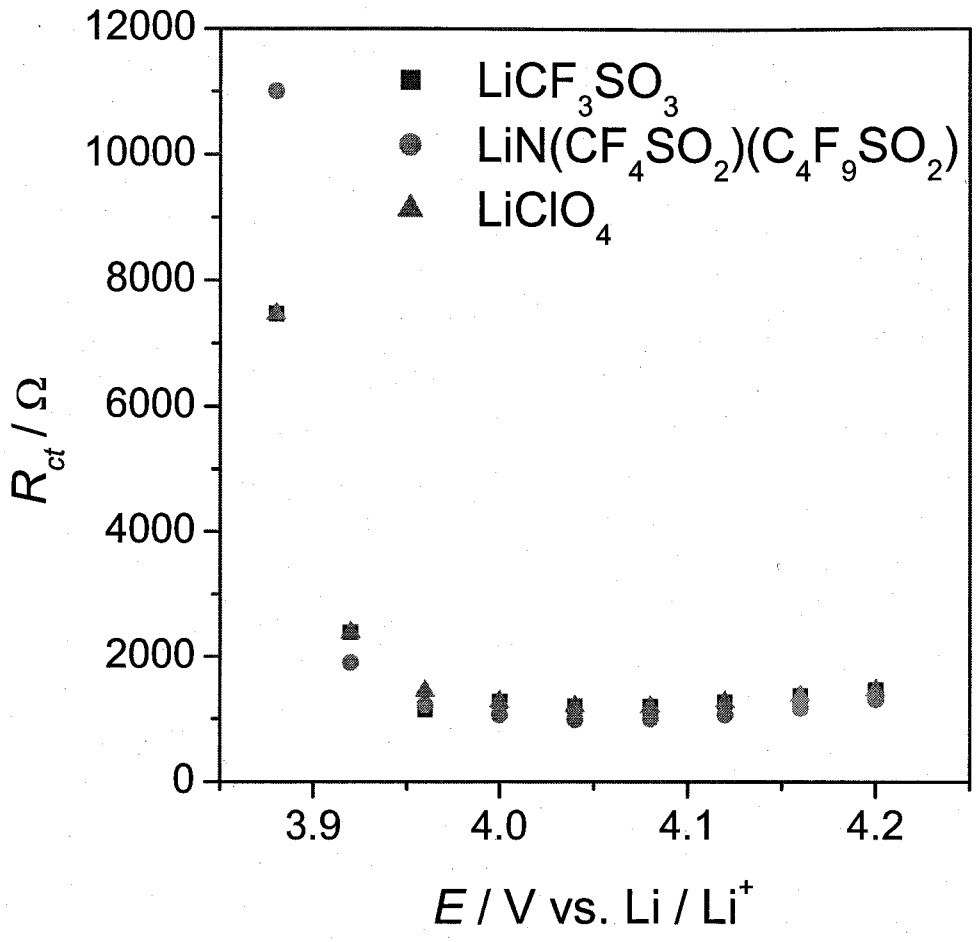

Fig 5.3. Variation of the charge transfer resistance for a $LiCoO_2$ thin film electrode / electrolyte interface with the electrode potential. Electrolytes are 1 mol dm^{-3} of ■; $LiCF_3SO_3$, ●;$LiN(CF_3SO_2)(C_4F_9SO_2)$, ▲; $LiClO_4$ in propylene carbonate.

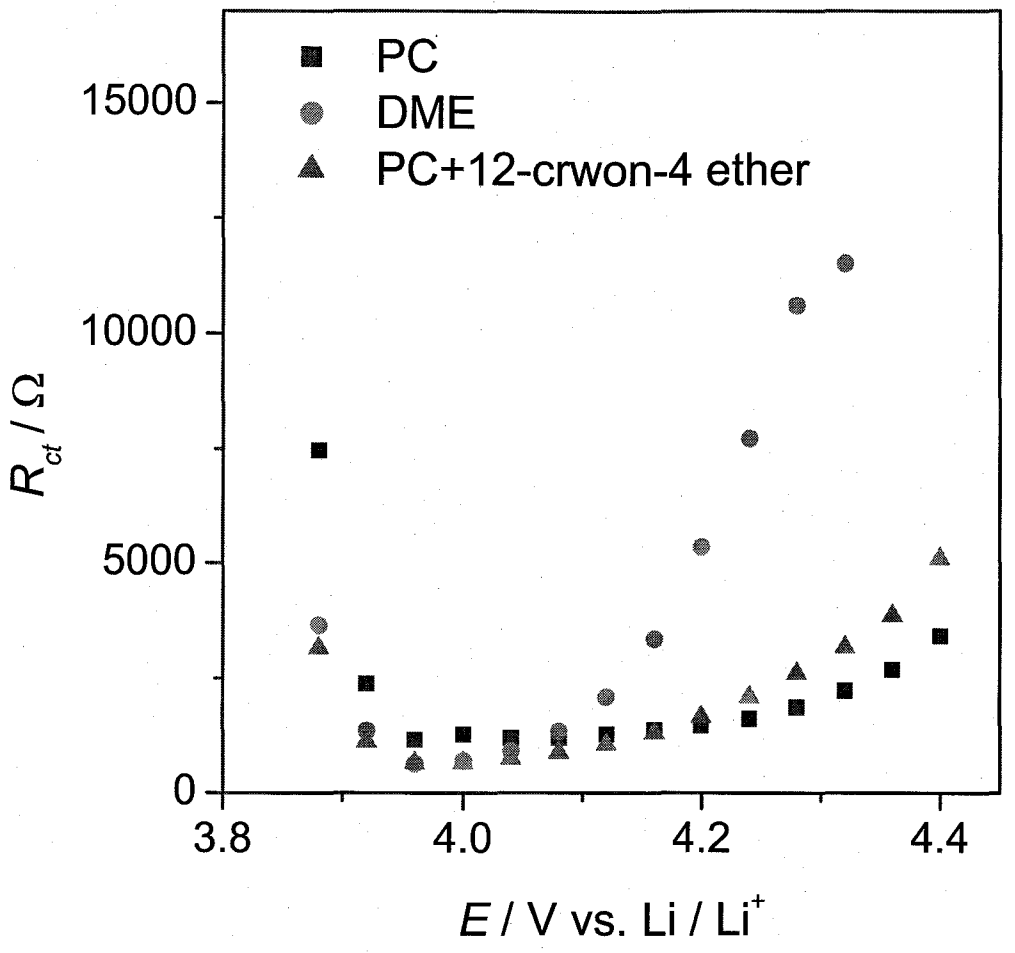

Fig 5.4. Variation of the charge transfer resistance for a $LiCoO_2$ thin film electrode / electrolyte interface with electrode potential. Electrolytes are ■; propylene carbonate, ●;dimethyl ether, ▲; propylene carbonate mixed with 12-crown-4 ether containing 1 mol dm^{-3} $LiCF_3SO_3$.

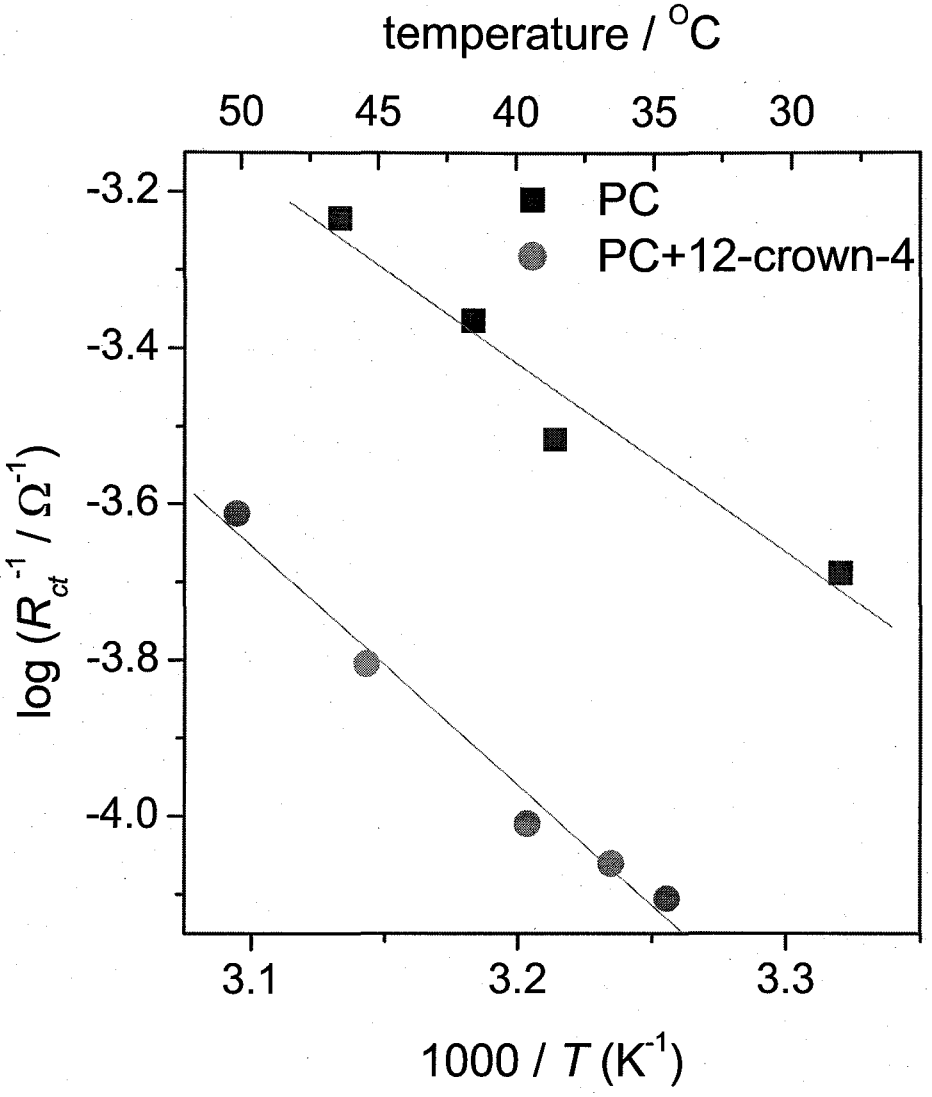

Fig 5.5. Temperature-dependence of the charge transfer resistance for a $LiCoO_2$ thin film electrode / electrolyte interface at 4.0 V. Electrolytes are ■; propylene carbonate, ●; propylene carbonate mixed with 12-crown-4 ether containing 1 mol dm^{-3} $LiCF_3SO_3$.

PUBLICATION LIST

PART I

CHAPTER 1

Lithium-Ion Transfer at $LiMn_2O_4$ Thin Film Electrode Prepared by Pulsed Laser Ablation

Izumi Yamada, Takeshi Abe, Yasutoshi Iriyama and Zempachi Ogumi

Electrochemistry Communications **5(6)** (2003) 502-505

CHAPTER 2

Lithium-Ion Transfer at Positive Electrodes / Electrolyte Interface – Effect of Positive Materials -

Izumi Yamada, Yasutoshi Iriyama, Takeshi Abe and Zempachi Ogumi,

Journal of Materials Research, submitted

CHAPTER 3

Lithium-Ion Transfer on Li_XCoO_2 Thin Film Electrode Prepared by Pulsed Laser Deposition – Effect of Orientation –

Izumi Yamada, Takeshi Abe, Yasutoshi Iriyama and Zempachi Ogumi

Journal of Power Sources, submitted

PART II

CHAPTER 4

Lithium Ion Transfer between Li_XCoO_2 and Polymer Gel Electrolyte

Izumi Yamada, Takeshi Abe, Yasutoshi Iriyama and Zempachi Ogumi

Science and Technology of Advanced Materials **7(6)** (2006) 519-523

CHAPTER 5

Lithium Ion Transfer at Positive Electrode / Electrolyte Interface

– Effect of Electrolytes -

Izumi Yamada, Takeshi Abe, Yasutoshi Iriyama and Zempachi Ogumi

Submitted for Publication